NASA/TP—2017-219384

Drawbar Pull (DP) Procedures for Off-Road Vehicle Testing

Colin Creager and Vivake Asnani
Glenn Research Center, Cleveland, Ohio

Heather Oravec
The University of Akron, Akron, Ohio

Adam Woodward
Virginia Polytechnic Institute, Blacksburg, Virginia

August 2017

NASA STI Program . . . in Profile

Since its founding, NASA has been dedicated to the advancement of aeronautics and space science. The NASA Scientific and Technical Information (STI) Program plays a key part in helping NASA maintain this important role.

The NASA STI Program operates under the auspices of the Agency Chief Information Officer. It collects, organizes, provides for archiving, and disseminates NASA's STI. The NASA STI Program provides access to the NASA Technical Report Server—Registered (NTRS Reg) and NASA Technical Report Server—Public (NTRS) thus providing one of the largest collections of aeronautical and space science STI in the world. Results are published in both non-NASA channels and by NASA in the NASA STI Report Series, which includes the following report types:

- TECHNICAL PUBLICATION. Reports of completed research or a major significant phase of research that present the results of NASA programs and include extensive data or theoretical analysis. Includes compilations of significant scientific and technical data and information deemed to be of continuing reference value. NASA counter-part of peer-reviewed formal professional papers, but has less stringent limitations on manuscript length and extent of graphic presentations.

- TECHNICAL MEMORANDUM. Scientific and technical findings that are preliminary or of specialized interest, e.g., "quick-release" reports, working papers, and bibliographies that contain minimal annotation. Does not contain extensive analysis.

- CONTRACTOR REPORT. Scientific and technical findings by NASA-sponsored contractors and grantees.

- CONFERENCE PUBLICATION. Collected papers from scientific and technical conferences, symposia, seminars, or other meetings sponsored or co-sponsored by NASA.

- SPECIAL PUBLICATION. Scientific, technical, or historical information from NASA programs, projects, and missions, often concerned with subjects having substantial public interest.

- TECHNICAL TRANSLATION. English-language translations of foreign scientific and technical material pertinent to NASA's mission.

For more information about the NASA STI program, see the following:

- Access the NASA STI program home page at http://www.sti.nasa.gov

- E-mail your question to help@sti.nasa.gov

- Fax your question to the NASA STI Information Desk at 757-864-6500

- Telephone the NASA STI Information Desk at 757-864-9658

- Write to:
  NASA STI Program
  Mail Stop 148
  NASA Langley Research Center
  Hampton, VA 23681-2199

NASA/TP—2017-219384

Drawbar Pull (DP) Procedures for Off-Road Vehicle Testing

Colin Creager and Vivake Asnani
Glenn Research Center, Cleveland, Ohio

Heather Oravec
The University of Akron, Akron, Ohio

Adam Woodward
Virginia Polytechnic Institute, Blacksburg, Virginia

National Aeronautics and
Space Administration

Glenn Research Center
Cleveland, Ohio 44135

August 2017

This report is a formal draft or working paper, intended to solicit comments and ideas from a technical peer group.

Level of Review: This material has been technically reviewed by expert reviewer(s).

Available from

NASA STI Program
Mail Stop 148
NASA Langley Research Center
Hampton, VA 23681-2199

National Technical Information Service
5285 Port Royal Road
Springfield, VA 22161
703-605-6000

This report is available in electronic form at http://www.sti.nasa.gov/ and http://ntrs.nasa.gov/

Contents

Drawbar Pull (DP) Procedures for Off-Road Vehicle Testing

Colin Creager and Vivake Asnani
National Aeronautics and Space Administration
Glenn Research Center
Cleveland, Ohio 44135

Heather Oravec
The University of Akron
Akron, Ohio 44325

Adam Woodward
Virginia Polytechnic Institute
Blacksburg, Virginia 24061

Summary

As NASA strives to explore the surface of the Moon and Mars, there is a continued need for improved tire and vehicle development. When tires or vehicles are being designed for off-road conditions where significant thrust generation is required, such as climbing out of craters on the Moon, it is important to use a standard test method for evaluating their tractive performance. The drawbar pull (DP) test is a way of measuring the net thrust generated by tires or a vehicle with respect to performance metrics such as travel reduction, sinkage, or power efficiency. DP testing may be done using a single tire on a traction rig, or with a set of tires on a vehicle; this report focuses on vehicle DP tests. Though vehicle DP tests have been used for decades, there are no standard procedures that apply to exploration vehicles. This report summarizes previous methods employed, shows the sensitivity of certain test parameters, and provides a body of knowledge for developing standard testing procedures. The focus of this work is on lunar applications, but these test methods can be applied to terrestrial and planetary conditions as well.

Section 1.0 of this report discusses the utility of DP testing for off-road vehicle evaluation and the metrics used. Section 2.0 focuses on test-terrain preparation, using the example case of lunar terrain. There is a review of lunar terrain analogs implemented in the past and a discussion on the lunar terrain conditions created at the NASA Glenn Research Center, including methods of evaluating the terrain strength variation and consistency from test to test. Section 3.0 provides details of the vehicle test procedures. These consist of a review of past methods, a comprehensive study on the sensitivity of test parameters, and a summary of the procedures used for DP testing at Glenn.

1.0 Introduction

1.1 Concept of Drawbar Pull (DP) Testing

DP testing has traditionally been used to evaluate the ability of a tractor to drag a farming implement. During the DP test the vehicle is driven with constant wheel velocity, and its forward motion is resisted by external force applied at its drawbar (a towing hitch). Exploration vehicles also need to be able to overcome external resistance in order to ascend slopes, accelerate, or tow equipment. Whereas tractors can be evaluated in the field, exploration vehicles must be evaluated in prepared terrain that represents the mobility challenges that are anticipated (see Figure 1).

During a DP test, the vehicle must generate sufficient tire-terrain thrust to overcome rolling resistance, and additional thrust to overcome the imposed DP force, F_{DP}. In soft soil, increases in DP force are directly related to increased wheel slippage and sinkage. With sufficient DP force, the vehicle's forward progress can be stopped; its wheels will spin in place, and the vehicle may become buried in the terrain. Through the complete range of F_{DP}, from zero (the vehicle's self-propelled condition) through the maximum F_{DP} (that which stops forward travel), vehicle performance is assessed in terms of metrics that relate to travel efficiency, energy usage, and immobilization.

For exploration vehicles, the DP test is used to characterize rather than predict performance. Predictive testing would require that the test terrain mimic field conditions, but this is generally impractical when an unexplored destination is being considered. Instead of predictive testing, characterization is done to compare vehicles or alternative vehicle configurations (e.g., changes to weight distribution, tires, or suspension) in several terrain types. Standardized and repeatable terrain

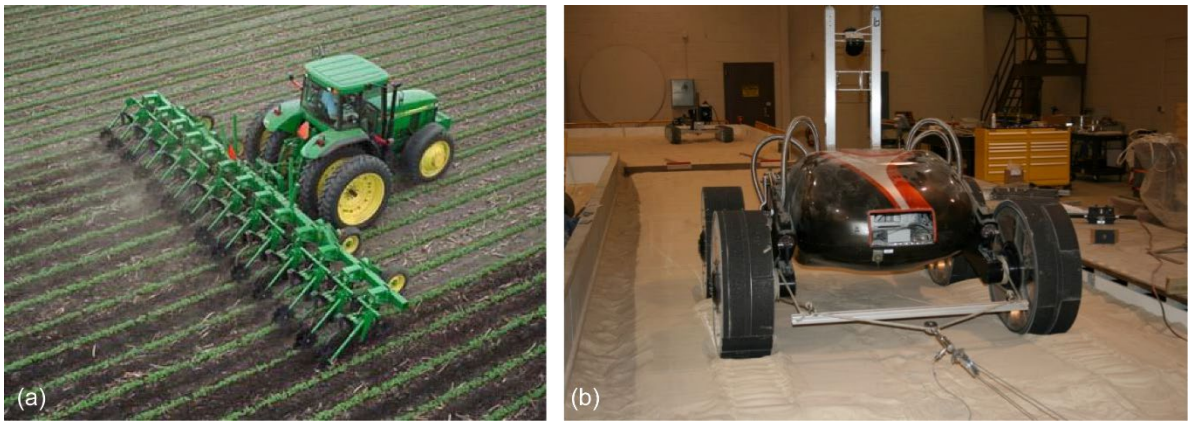

Figure 1.—Drawbar pull (DP) tests in farming and exploration vehicles. (a) Farming tractor towing a drawbar load. (b) Exploration vehicle undergoing DP testing.

conditions are used, with each terrain type emphasizing different characteristics (e.g., low bearing strength, high cohesion, and high friction). This allows a vehicle to be purposefully configured for mobility over a range of conditions that encompass those believed to be in the exploration site.

1.2 Objectives and Organization of the Manuscript

A standard exists for DP test procedures specific to earth-moving machinery (International Organization for Standardization, 1983); however, it lacks information necessary for evaluating the performance of wheels and/or vehicles for exploration purposes. The primary objective when conducting DP tests on earth-moving machinery, such as construction or agricultural vehicles, is to determine the maximum allowable towing force at each drive train configuration. These tests are typically done in the field on unprepared (but hard) terrain at low slip. For exploration purposes, other factors such as travel safety, speed, and efficiency are important. In addition, exploration vehicles, especially those intended for the Moon, are likely to encounter a variety of difficult terrain conditions, including dry loose soil. Because of this, it is important to evaluate the wheels or vehicles in a controlled terrain that simulates these challenges and to observe their behavior along a greater range of wheel slip. Lacking a universally accepted standard that is specific to exploration vehicles, those who wish to use DP testing methods must resort to trial and error.

Over the course of several years, the NASA Glenn Research Center has developed procedures for DP testing of exploration vehicles, and these procedures continue to be refined. It is the objective of this report to explain the procedures that are used at Glenn and to contrast them with other reported methods. The authors' intent for providing this information is to make it easier for others to implement the DP test and to contribute to the development of standard practices.

The final subsection of this Introduction (Section 1.3) is an explanation of the metrics and meaning of DP data. The body of this report consists of sections on terrain preparation (Section 2.0) and test method development (Section 3.0). Terrain preparation is not a subject that can be generalized easily; therefore, it is presented as a case study on the development of terrain for testing lunar vehicles. Both sections include discussions of methods that are reported in the literature, the methods used at Glenn, and how the methods at Glenn were selected. The report concludes with a series of suggestions to improve upon these methods and appendixes that define the symbols used in this report (Appendix A), outline the entire DP testing procedure (Appendix B), provide sample data sheets (Appendix C), and provide sample DP test data (Appendix D).

1.3 Test Variables

1.3.1 Applied Drawbar Pull (DP) Force

During the test, DP is applied to the vehicle at a specified hitch point. Figure 2 shows a simplified free-body diagram of a 4×4 vehicle during a DP test. The DP force, F_{DP}, may be equated to the other forces involved as follows:

$$F_{DP} = F_{rear} + F_{front} - R_{rear} - R_{front} - ma \tag{1}$$

where F is force, R is resistance, m is mass, a is acceleration, and the subscripts front and rear indicate the front and rear axles. For a vehicle with an arbitrary number of axles this is generalized as

$$F_{DP} = \sum F_{axles} - \sum R_{axles} - ma \tag{2}$$

The term "axle" is used to describe a pair of wheels with identical driving conditions and at the same location along the length of the vehicle (e.g., both of the front wheels together would be the "front axle"). It is assumed for the types of tests described in this report that the left and right sides of the vehicle

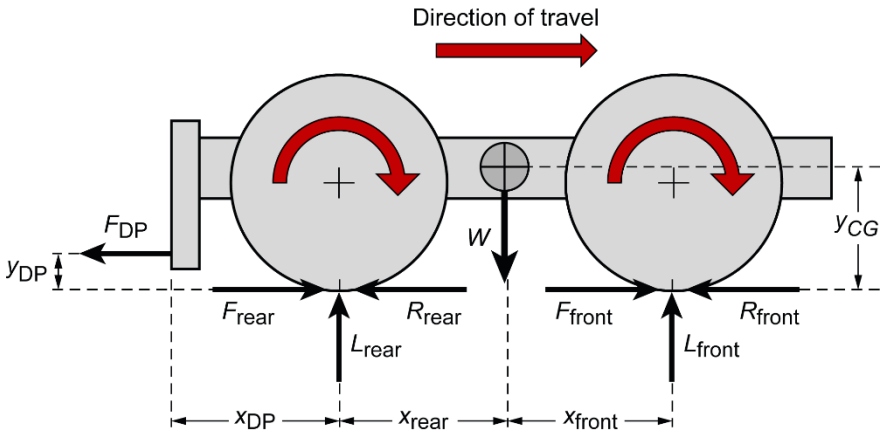

Figure 2.—Forces and moments acting upon a 4×4 vehicle during a drawbar pull (DP) test. *F*, force; *L*, normal load; *R*, resistance; *W*, vehicle weight; *x*, horizontal distance; *y*, vertical distance. Subscripts: rear and front, rear and front tires and axles; *CG*, center of gravity.

encounter the same terrain conditions and perform the same. This allows the forces acting on the vehicle to be represented in two dimensions.

Each axle generates forward thrust, which is used to overcome resistances associated with the soil and tire deformation as well as the drawbar and acceleration forces on the vehicle body. If the travel velocity is constant, the applied F_{DP} is equivalent to the vehicle's net thrust or the thrust generated in excess of motion resistance.

1.3.2 State Variables: Slip and Travel Reduction

The metrics of slip *i* and travel reduction *TR* have several different interpretations, and in some cases, the terms are used interchangeably (Meyer et al., 1977, ASAE, 2003). Here slip is used to quantify the shear displacement beneath a wheel, while *TR* represents the associated reduction in the forward progress of the vehicle. The metrics use the same mathematical expression,

$$\{i \text{ or } TR\} = \frac{v_{ref} - v}{v_{ref}} \tag{3}$$

which is a normalized comparison between forward velocity *v* and a predetermined reference velocity v_{ref}. Equation (3) is rearranged as Equation (4) to show that the reference velocity is equal to the forward velocity when *i* or *TR* is zero. Consequently, an experimental "zero condition" is established for each metric in order to measure the reference velocity (ASAE, 2003). For example, the U.S. Army Waterways Experiment Station (WES) (McRae et al., 1965) used the velocity on hard ground as the v_{ref} when computing slip.

$$v_{ref} = \left.\frac{v}{1-\{i \text{ or } TR\}}\right|_{\{i \text{ or } TR\}=0} = v \tag{4}$$

This framework is used to explain the meaning of *i* and *TR* in the following paragraphs:

Slip: Slip is associated with a single wheel (or single traction device) and is used as an indicator of shear displacement. The zero-condition corresponds to driving a wheel on the test-terrain with minimal shear displacement. The zero condition is usually established with a special-purpose single-wheel testing machine. The machine drives the wheel with fixed angular velocity, and the forward velocity is adjusted until minimal shear displacement is observed. The forward velocity under these conditions is then considered the reference velocity used to calculate slip. The slip metric has been used extensively in single-wheel validation experiments, because terramechanics models often use slip as a part of their mathematical framework. However, a known limitation of this metric is that the determination of the zero condition is often subjective. The following references discuss this issue: Sharma and Pandey (1998), Wong (2010), Schreiber and Kutzbach (2007), and Gill and Vanden Berg (1968).

TR: Travel reduction is associated with the test vehicle and is used to observe changes in forward progress as slip occurs. The zero-condition is not based on a specific physical phenomenon; rather it is selected to be a simple and repeatable experimental condition. For self-powered vehicles, such as exploration rovers, there are two common zero conditions (ASAE, 2003): (1) self-propelled (zero F_{DP}) on hard ground and (2) self-propelled on the test terrain. Driving on hard ground is more repeatable, and it provides a logical basis to compare with soft-terrain driving. However, the self-propelled condition in the test terrain is a more convenient choice when DP testing is conducted in the field. Travel reduction results must always be interpreted as relative to whatever zero condition has been selected. However, the absolute values of *TR* become

significant when they are correlated with the vehicle performance metrics observed during the DP test.

Often the reference velocity is redefined as a function of the angular wheel velocity ω as follows,

$$v_{\text{ref}} = r_r \omega \tag{5}$$

where the proportionality constant r_r is called the rolling (or effective) radius. The *i* and *TR* equation then becomes

$$\{i \text{ or } TR\} = \frac{r_r \omega - v}{r_r \omega} \tag{6}$$

Equation (6) is rearranged as Equation (7) to show that rolling radius is simply the forward velocity normalized by the angular velocity when the vehicle is operating at the zero condition.

$$r_r = \left.\frac{v}{\omega\left(1-\{i \text{ or } TR\}\right)}\right|_{\{i \text{ or } TR\}=0} = \frac{v}{\omega} \tag{7}$$

Using the rolling radius framework is convenient because it allows for *i* and *TR* to be determined even when the angular wheel velocity differs from the zero-condition experiment. It should be noted, however, that this formulation assumes that the rolling radius is a velocity-independent quantity.

For DP testing, *i* and *TR* are used as state variables because they are easily measured and have a strong correlation with performance metrics. For example, vehicle DP testing may show that 60-percent *TR* results in a net tractive force equal to 27 percent of the vehicle weight but that peak tractive efficiency occurs at 9-percent *TR* (see Figure 3 and Figure 4). Mapping between either *i* or *TR* enables the performance of a vehicle in the field to be inferred from the velocity measurements.

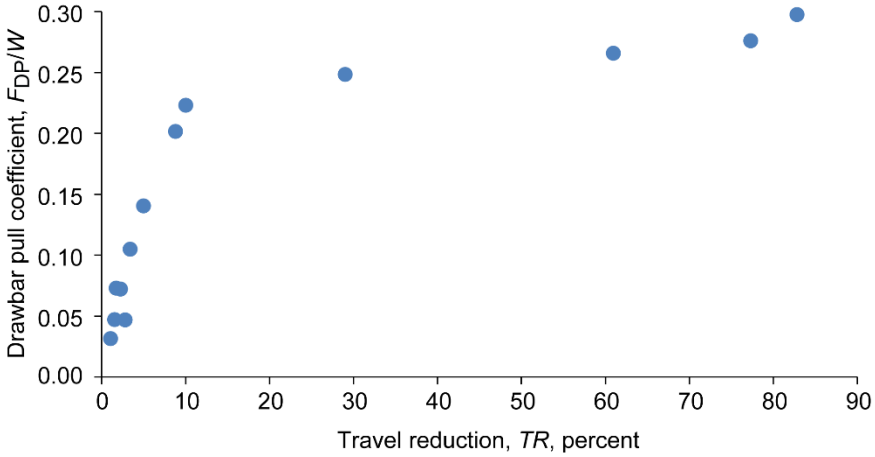

Figure 3.—Sample plot of travel reduction versus drawbar pull (DP) coefficient.

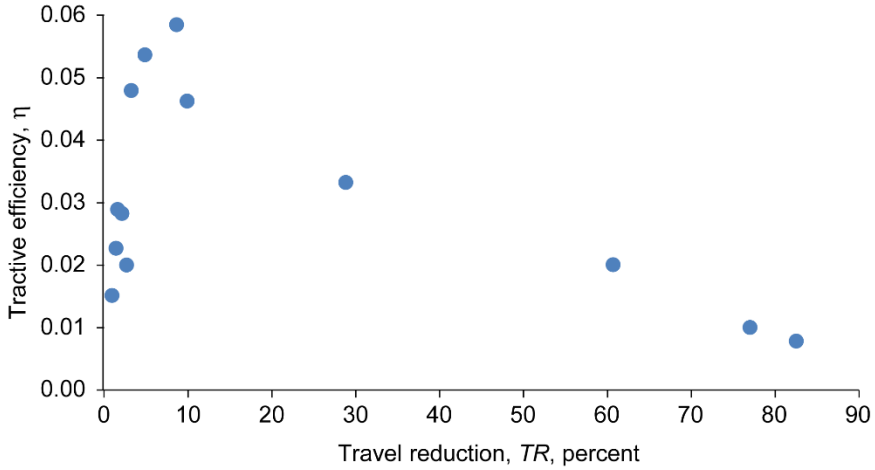

Figure 4.—Sample plot of travel reduction versus tractive efficiency.

TABLE I.—COMPARISON OF SLIP AND TRAVEL REDUCTION FOR VEHICLE EVALUATION

Evaluation factor	Slip, *i*	Travel reduction, *TR*
Represents a true physical interpretation.	Yes	No
Rolling radius can be measured without a single-wheel test machine.	No	Yes
Rolling radius may be independent of terrain.	↓	↓
Results from different terrain conditions and laboratories can be compared readily.		
Full vehicle response is captured.		

There are some key advantages and disadvantages to using *i* or *TR*, as outlined in Table I. Slip tends to have a more useful physical interpretation, because it is anchored to a specific terrain condition. On the other hand, travel reduction has many practical advantages. A single-wheel test machine is not required for finding the rolling radius. The value of rolling radius does not change with the test terrain. This means that separate rolling radius measurements are not needed to interpret test results in a new terrain and that *TR* may be more readily used for monitoring a vehicle in the field. If driving on hard ground is used as the reference condition, the *TR* measured in different terrains and laboratories may be compared easily. Finally, *TR* provides a single number to capture the full vehicle state. This is not always an advantage, but it makes this metric easier to use.

For the practical reasons outlined here, *TR* is the state variable that is most commonly used for vehicle DP testing at Glenn. Unless there are special circumstances, the reference condition is the test vehicle traveling on hard ground that is covered with a nonslip surface, with the vehicle's weight distribution equivalent to the DP test conditions.

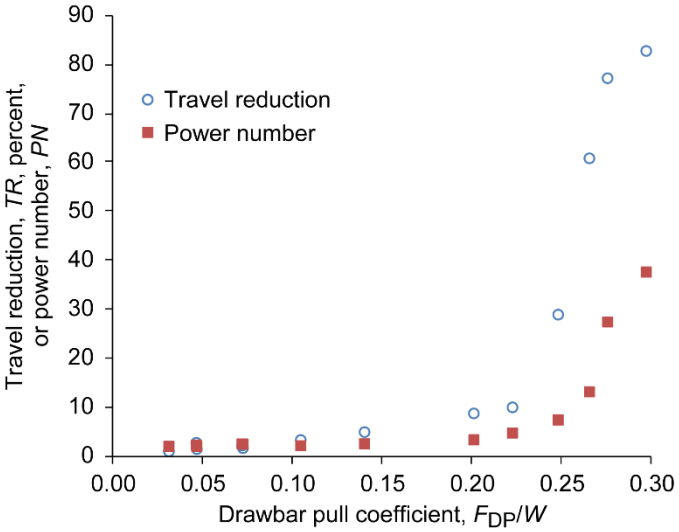

Figure 5.—Results of drawbar pull (DP) test, displaying travel reduction and power number as functions of the DP coefficient.

1.3.3 Performance Metrics

Performance metrics for the DP test follow:

DP *coefficient, F_{DP}/W:* *The applied* DP *force normalized by the vehicle's overall weight.*—The DP coefficient is most often used as an independent variable when the other performance metrics are being evaluated. The normalization allows for vehicles of dissimilar weight to be compared.

Travel reduction, TR: *A measure of travel efficiency, as defined in Equation (3), where lower values are associated with increased vehicle velocity.*—As mentioned in the previous section, travel reduction also is used as a state variable to indicate vehicle performance. Figure 4 shows an example of *TR* as a state variable, and Figure 5 shows *TR* as a function of F_{DP}/W.

Sinkage, z: *A measure of a wheel's depth below the terrain surface.*—Increases in wheel sinkage relate to an increased risk for vehicle immobilization. Sinkage also can be normalized by the wheel radius and represented as a unitless value (see Figure 6).

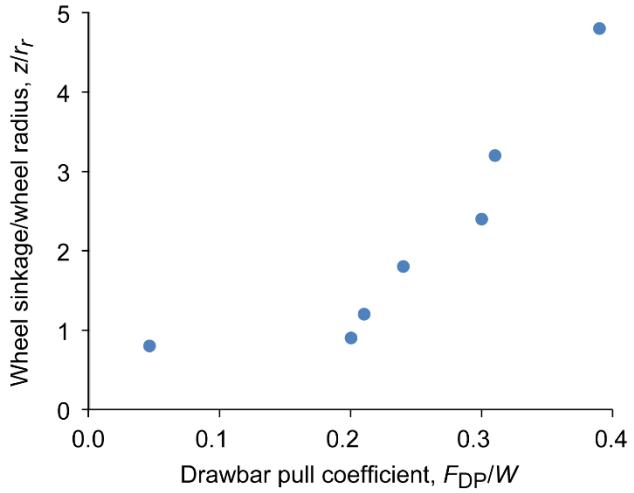

Figure 6.—Sample plot of wheel sinkage normalized by wheel radius.

Power number, PN: *A unitless metric used to quantify the power and energy costs of mobility.*—It is defined as the power being used normalized by the vehicle's weight and velocity (Meyer et al., 1977). Normalization allows for vehicles of different weight and travel velocity to be compared.

$$PN = \frac{P}{Wv} \tag{8}$$

Another way to interpret this metric is the energy consumed E per unit of distance traveled d per unit of vehicle weight (Freitag et al., 1970).

$$PN = \frac{E}{Wd} \tag{9}$$

To isolate the mobility system, one should compute the power from the measured mechanical torque and speed of the running gear. When the vehicle is considered as a system, the power should be measured at the source, such as the power delivered by the battery of an electric vehicle. A PN versus F_{DP}/W chart is useful for mission planning because it can be used to estimate the power and energy required to travel in a specific terrain with an external load (e.g., grade resistance). For power to be computed, the PN must be multiplied by the vehicle weight and forward velocity. For the energy to be found, the PN must be multiplied by the vehicle weight and travel distance. Figure 5 provides an example of PN data as a function of TR.

Tractive, or drawbar, efficiency, η: *A unitless metric representing the efficiency of transferring power to move an external load.*—It is defined (Meyer et al., 1977) as the ratio of DP force and velocity to the vehicle power:

$$\eta = \frac{F_{DP}v}{P} \tag{10}$$

Tractive efficiency will drop to zero when zero drawbar load is applied, as well as when there is enough drawbar load to create zero forward velocity. There is typically an optimum DP load between these values that maximizes this metric. As a result, tractive efficiency is used to optimize towing by adjusting the towing load or vehicle configuration to operate at peak efficiency. See Figure 4 for an example of a tractive efficiency plot.

2.0 Terrain Preparation

2.1 Simulating Lunar Terrain Strength

With the development of surface vehicles for exploration and construction operations on the Moon (National Aeronautics and Space Administration (2008a, b), there is a need to characterize the tractive performance of lunar vehicles in terrain that responds similar to the lunar terrain. In general, terrain deformation in response to vehicle loading is controlled by the composition and compactness of the surface material, atmospheric conditions, and gravity. The greater part of the lunar surface is believed to be covered by finely reworked, highly fractured, dry regolith material consisting predominately of impact melt breccias and agglutinates (McKay et al., 1991). The mean particle size distribution (of the subcentimeter fraction of the regolith) ranges from 40 to 800 μm, with the majority averaging between 60 and 80 μm (McKay et al., 1991). The individual particles range in shape from round to elongated and subangular to angular (Carrier et al., 1991). In addition, the bulk density of the lunar regolith is estimated to range from 1.53 to 1.63 g/cm^3 in the first 30 cm of depth (Carrier et al., 1991). The friction angle is estimated to range between 30° and 50°, and small amounts of cohesion up to 1 kPa have been observed (Carrier et al., 1991).

Lunar soil simulants such as MLS–1, JSC–1, and JSC–1A have been developed to approximately represent the elemental composition and chemistry of the lunar regolith in specific regions (Batiste and Sture, 2005; Carter et al., 2004; Klosky et al., 1996; Zeng et al., 2010). Theoretically they could be used for large-scale vehicle testing here on Earth, but relatively small quantities of these simulants are available. Also it would be impractical to control the atmospheric conditions (e.g., vacuum and gravity) necessary for these simulants to exhibit mechanical strength similar to that of lunar soil. Accordingly, a new lunar strength simulant, Glenn Research Center 1 (GRC–1), was developed at Glenn specifically for terramechanics testing in Earth ambient conditions (Oravec et al., 2010). The proper preparation of this material has been shown to result in terrain strength representative of the lunar terrain as validated by lunar surface cone penetration (CPT) measurements (Mitchell et al., 1972a,b; National Space Science Data Center, 2005), but on the conservative end of driving difficulty. The preparation procedures for establishing the target terrain conditions using GRC–1 are discussed in detail here, starting with a review of past work on terrain preparation.

2.2 Review of Past Work on Terrain Preparation and Measurement

2.2.1 Cone Penetrometer as a Tool for Evaluating Terrain Strength

Over the years, numerous instruments have been developed with the objective of measuring terrain properties that correlate with vehicle mobility performance. For instance, the Fighting Vehicles Research and Development Establishment in England used a vane shear apparatus to obtain in situ shear strength (Smith, 1964). Alternatively, the Land Locomotion Laboratory, Detroit Arsenal, used M.G. Bekker's bevameter to obtain the load-displacement characteristics of the terrain surface in both

compression and shear (Bekker, 1960). From these stress-strain relationships, parameters can be derived that are used to describe the behavior of the terrain in response to vehicle loading (Bekker, 1960; Janosi and Hanamoto, 1961).

In contrast, WES used the cone penetrometer to obtain a single terrain-strength index that is representative of bearing capacity, compressibility, shear strength, and interface friction (U.S. Army, 1948). The following is a brief summary of the history and functionality of the cone penetrometer:

- The cone penetrometer in situ soil-testing device was originally introduced in the field of terramechanics by WES during World War II in 1945. It was designed as a quick and easy way to determine the capability of off-road army vehicles to safely traverse a given terrain (U.S. Army, 1948).
- The simple CPT test is a method by which the in situ strength or consistency of soils can be measured; the force required to maintain a constant rate of penetration is regarded as a measure of the consistency of the soil, known as the cone penetration resistance, or cone index (*CI*).
- The *CI* is defined as the force per unit area that is required to push a cone with an apex angle of 30° and a base area of 323 mm^2 (0.5 in^2) through a soil at a rate no greater than 2 cm/s. These parameters define the "standard" WES cone penetrometer.
- The value of the *CI* represents a combination of soil properties including bearing capacity, compressibility, shear strength, and interface friction. The *CI* cannot be used to identify specific properties of the soil such as cohesion or the angle of internal friction unless the soil is purely cohesive (clay) or purely frictional (sand). For example, Freitag et al. (1970) clearly explain that in a purely frictional soil, the resistance to penetration is a function of the confining pressure resulting from the weight of the soil above the point being measured and the friction angle of the soil, both of which are recognizably dependent on the density of the soil.
- A common metric associated with the cone penetrometer is the cone penetration resistance gradient, also known as the cone index gradient *G*. The cone index gradient is used to represent the rate of penetration resistance increase averaged over the depth of measurement (see Figure 7 for sample CPT data). In other words, it is the slope of the resulting penetration-resistance-versus-depth curve.

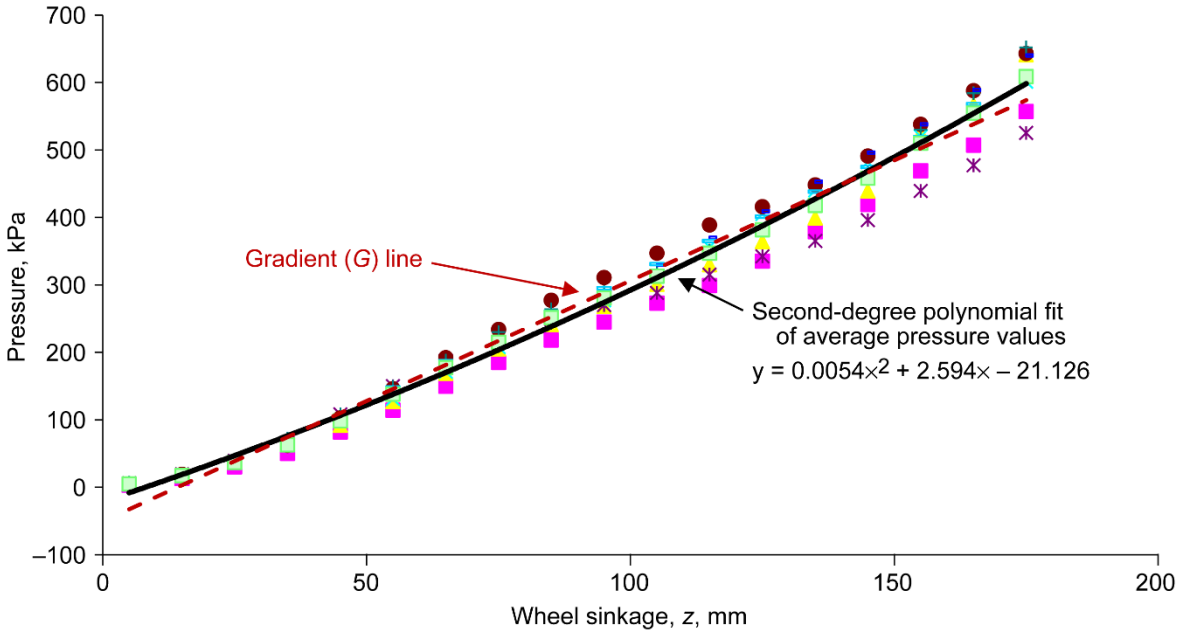

Figure 7.—Typical cone penetrometer results for the T2 terrain condition. Eight data sets are shown together with a second-degree polynomial fit of the average penetration-resistance-versus-depth data points. Cone index gradient, *G* = 3.57 kPa/mm; standard deviation = 0.286 kPa/mm; linearity coefficient = 0.0054 kPa/mm^2.

Although other geotechnical tools are used at Glenn to acquire specific soil properties in a controlled laboratory, the cone penetrometer was chosen as the standard tool to evaluate the in situ terrain conditions for the following reasons:

- Cone penetrometer data were taken of the Moon's surface during the Apollo 15 and 16 missions (National Space Science Data Center, 2005), thus the terrain prepared for testing at Glenn can be correlated to the lunar terrain with respect to the cone index gradient.
- When conducting the DP tests at Glenn, the researchers did not intend to derive terrain data for modeling purposes but rather to quantify the strength condition and examine variation between locations and from test to test. The cone penetrometer serves this function very well.
- The cone penetrometer is inexpensive, compact, and readily available commercially.
- For a specific material, the cone index gradient can be correlated with bulk density. This can then be used to map *G* to other mechanical soil properties.

2.2.2 Measurement of Terrain Strength and Development of Parametric Relations

As verified at Glenn, and discussed in Section 3.0, the cone index gradient has a direct correlation with vehicle mobility in a dry granular soil (Green, 1967). Though the specific properties of a soil cannot be derived solely with the cone penetrometer, the cone index gradient does provide comparative information on how a vehicle will interact with the terrain. For example, a vehicle will typically sink less on a terrain that has a high cone index value than one with a low index value, assuming that both terrains consist of similar types of material. This is the basis for using the lunar surface *G* values (National Space Science Data Center, 2005) to help determine a range of acceptable terrain strength for simulating the lunar surface on Earth. The lunar simulants used for vehicle testing can be conditioned to produce cone index gradient values similar to those taken on the Moon.

For a given dry granular soil, the cone index gradient depends on the relative density. Melzer (1971) investigated the relationship between the CPT gradient and the relative density of sands with various grain size distribution and compactibility. Melzer was able to show that quantitative relations between relative density and average cone index gradient could be established for these specific sand types. Because relative density can be correlated with the other properties of a soil, such as friction angle, *G* can also be used to estimate the in situ soil properties. This makes possible the translation of the systems of measurement between various organizations concerned with similar research, especially vehicle mobility.

2.2.3 Soil Preparation and Evaluation for Vehicle Mobility Studies

With the establishment of relations between CPT gradient and relative density it became easy to determine the repeatability of terrain preparation in laboratory vehicle mobility studies. Freitag et al. (1970) utilized the cone penetrometer in evaluating wheels for lunar vehicles. In this investigation, single-wheel and 4×4 vehicle tests were performed on an air-dry poorly graded sand (classified as SP–SM using the Unified Soil Classification System (USCS)) from the desert near Yuma, Arizona. For mobility testing, this soil was prepared as uniformly as possible in test bins measuring 8.25 m in length, 1.63 m in width, and 0.81 m in depth. The method of soil preparation included filling the test bin with soil and then plowing the top 0.3 m (12 in.) with a seed fork. For loose terrain conditions, no further manipulation of the soil was required and the surface of the plowed soil was leveled with a screed prior to testing. Denser terrain conditions were achieved through applying a vibrator to the soil surface after plowing and then screeding the soil level. The degree of vibratory compaction was based on the desired density of the terrain.

The uniformity of the soil in both loose and compacted conditions was evaluated with the standard WES cone penetrometer (323-mm^2 base area, 30° cone tip). For each CPT test the cone index gradient was calculated over the range of 4 to 19 cm in depth (measured from the cone tip). A total of five CPT tests were performed down the center line of the test bin prior to each single-wheel test. These data were averaged to determine the mean cone index gradient of the terrain before each test. The results for both cases are listed in Table II. This method of utilizing the cone penetration gradient for evaluating the uniformity of prepared test soils for mobility studies was continued by WES in later vehicle mobility investigations (Green and Melzer, 1970, 1971; Freitag et al., 1970).

2.3 Properties of Lunar Strength Simulant GRC–1

The lunar soil strength simulant used in this study, GRC–1, has been described in detail by Oravec et al. (2010). In brief, it is a blend of four different silica sand products from the Best Sands Corp of Chardon, Ohio. The grain size distribution of

TABLE II.—CONE PENETROMETER RESULTS FOR YUMA SAND
[Freitag et al., 1970.]

Terrain condition	Mean gradient, kPa/mm	Standard deviation, kPa/mm
S1	0.5432	0.0306
S2	3.0669	0.2636

the mixture approximates the coarse fraction (barring the <75-μm-diameter particles) of the mean lunar regolith particle size distribution (Carter et al., 2004). It is classified as poorly graded sand, SP, according to the USCS. Particle size distribution, represented by the particle size (in mm) versus percent finer by weight, and classification data are provided in Figure 8. The relation between the air-dry bulk density and relative density of GRC–1 is shown in Figure 9.

GRC–1 is considered to be a cohesionless soil with strength dominated by the frictional component. This simulant was developed utilizing cone penetration data from Apollo Missions 15 and 16 (Mitchell et al., 1972a, b; National Space Science Data Science, 2005) to calibrate a testbed for lunar vehicle mobility experiments. A summary of average cone index gradient values calculated from the lunar cone index data provided by the National Space Science Data Center (2005)

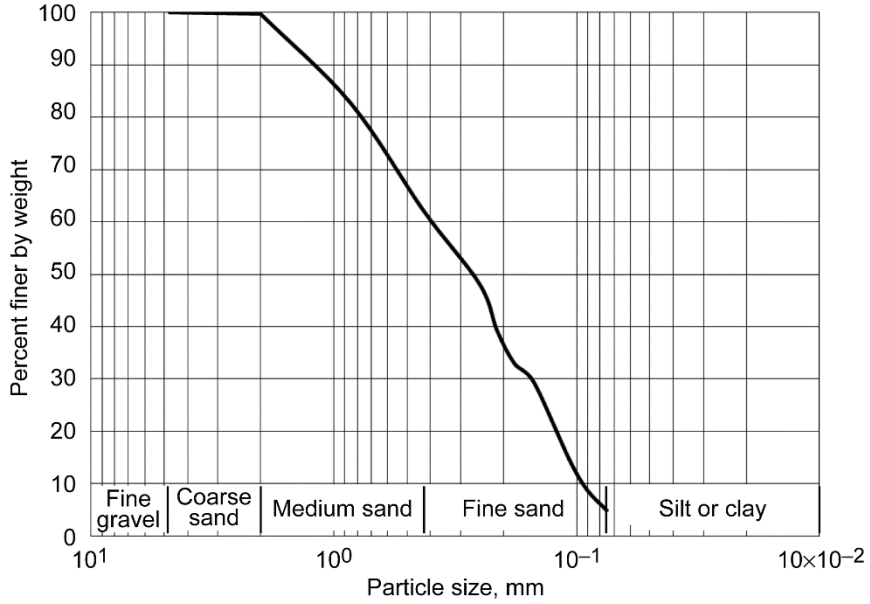

Figure 8.—Grain size distribution and soil properties of Glenn Research Center (GRC–1).

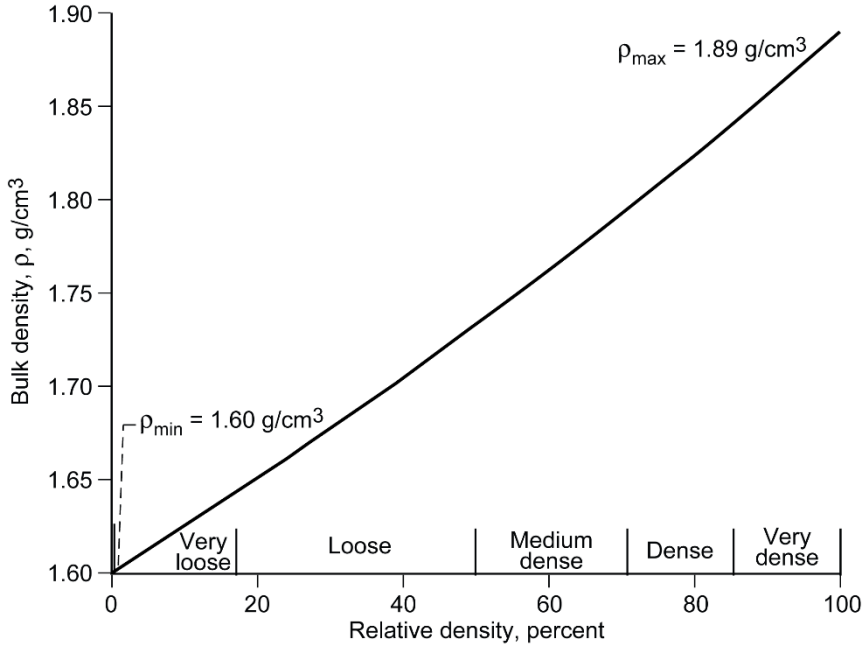

Figure 9.—Relation between air-dry bulk density and relative density of Glenn Research Center 1 (GRC–1).

TABLE III.—LUNAR TERRAIN CONE INDEX GRADIENT MEASUREMENTS NEAR APOLLO 15 AND 16 LANDING SITES

Mission	Location	Penetration depth, cm (Mitchell et al., 1972a, b)	Cone index gradient, *G*, kPa/mm (Oravec et al., 2010)
Apollo 15	Adjacent to trench	8.25	4.80
Apollo 15	In LRV track[a]	5.25	5.08
Apollo 15	Adjacent to LRV track[a]	<11.25	11.31
Apollo 16	Uphill, top of crater	20	3.32
Apollo 16	Near LRV track[a]	8	2.22

[a]LRV, Lunar Roving Vehicle.

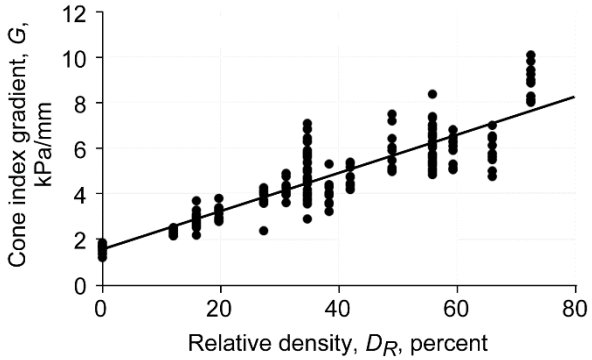

Figure 10.—Relation between relative density and cone index gradient of air-dry Glenn Research Center 1 (GRC–1). $G = 0.0834(D_R) + 1.5811$.

measured near the Apollo 15 and 16 landing sites is provided in Table III. As stated in Oravec et al. (2010), the design approach for GRC–1 assumes that if a dry granular terrain mimics the measured lunar cone penetration observations, as indicated by *G*, then the material will respond similarly to vehicle loading in terms of compaction and shear resistance.

In a previous study, the relation between the cone index gradient and relative density of air-dry GRC–1 was established on the basis of over 180 cone penetration tests conducted specifically for this purpose (Oravec et al., 2010). This relation, shown in Figure 10, is considered to be very reliable up to 80-percent relative density. For comparison with the lunar terrain, in Figure 11 the range of computed cone index gradient values from the National Space Science Data Center data set was plotted with the GRC–1 data. The results show that over its range of density, and in Earth ambient conditions, GRC–1 covers four of the five lunar terrain cone index gradient values. The value that cannot be simulated is a relatively high terrain strength: a condition that does not pose a challenge for vehicle mobility. Results from supplementary soil tests performed during previous investigations of this material, including triaxial, normal bevameter, and shear bevameter tests, can be found in Oravec et al. (2010).

2.4 Methods for Terrain Preparation

Glenn houses a 12- by 6- by 0.3-m soil bin with a 7- by 5- by 0.3-m adjustable tilt bed (0° to 45°) for vehicle testing in horizontal straight-line runs or sloped runs (Figure 12). In this bin, the flatbed portion was divided into two lanes of equal width. One lane was filled with GRC–1 for drawing pull evaluation. This lane measured 12 by 3 m and was prepared to a depth of approximately 0.30 m (12 in.). Because of the size of both bins, the soil had to be processed in place for each test. Because an automated mechanical system was not available, it would have been unrealistic to manually remove the soil from the bin and replace it in a systematic fashion for each test to have a repeatable method of preparing a homogeneous terrain. As an alternative, several manual methods for preparing the terrain in situ were attempted and evaluated. Test methods needed to be efficient and to provide a high degree of homogeneity and repeatability. Each method typically required three stages: (1) loosening the soil to return it to its original condition, (2) leveling to even out the soil distribution, and (3) compacting the soil to the desired strength as indicated by cone index gradient measurements. A discussion on how these stages are achieved at Glenn follows.

2.4.1 Loosening the Soil

For the terrain to be consistent for each test, the soil must be returned to its original loosened state. Otherwise, the compaction will have a cumulative effect on the terrain and the density will increase over time. The best way to ensure proper loosening is to remove the soil and then replace it in the soil bin

at a slow and steady rate. However, this was impractical for the large soil bin used, so a method using shovels to break up the soil was developed. It should be noted that most of the terrain preparation photos shown here (Figure 13 and Figure 14) are not of the soil bin at Glenn used for vehicle testing but of a smaller soil bin used for demonstrations.

(1) Begin by inserting a flat-blade shovel into the soil with the blade of the shovel perpendicular to the soil surface (Figure 13(a)). Maintain this angle until the shovel is inserted through the soil to the shovel's maximum depth (approximately 25 cm).

(2) Once the shovel reaches this depth, gently pull back (toward you) on the handle to lift the soil in front of the shovel, breaking up the soil particles. Pull the shovel back to an angle of approximately 45° from the vertical (Figure 13(b)).

(3) At this point return the shovel to its upright position (by pushing the handle away from you) and gently lift it out of the soil. This process creates two distinct features in the soil: a mound and a valley as labeled in Figure 13(c).

(4) To repeat this procedure, reinsert the shovel into the soil a distance equal to approximately half the shovel depth (12 to 13 cm) behind the valley that was formed by the previous insertion (Figure 13(c)). Repeat this process in a straight line, overlapping about 25 percent each time (Figure 13(d)), until an area at least twice as wide as the wheel track has been loosened. After loosening, the soil should look similar to Figure 13(e).

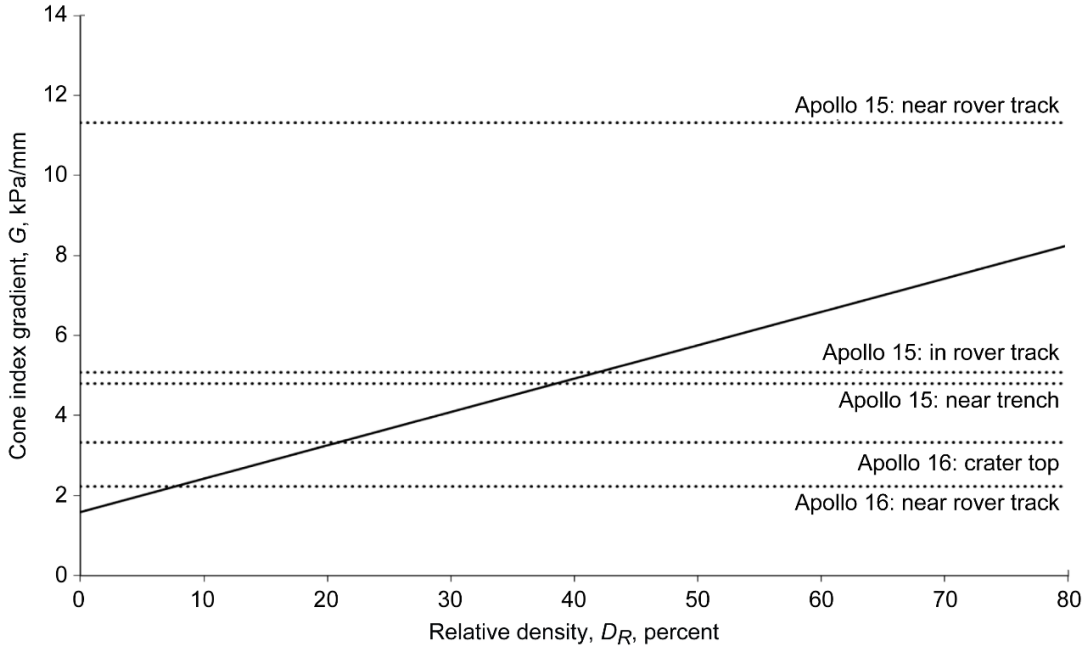

Figure 11.—Glenn Research Center 1 (GRC–1) cone penetration data compared with Apollo 15 and 16 cone index gradient values.

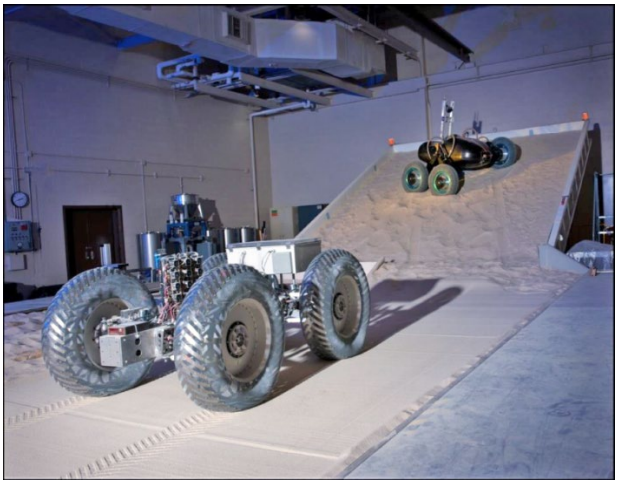

Figure 12.—NASA Glenn Research Center soil bed with tilt bed.

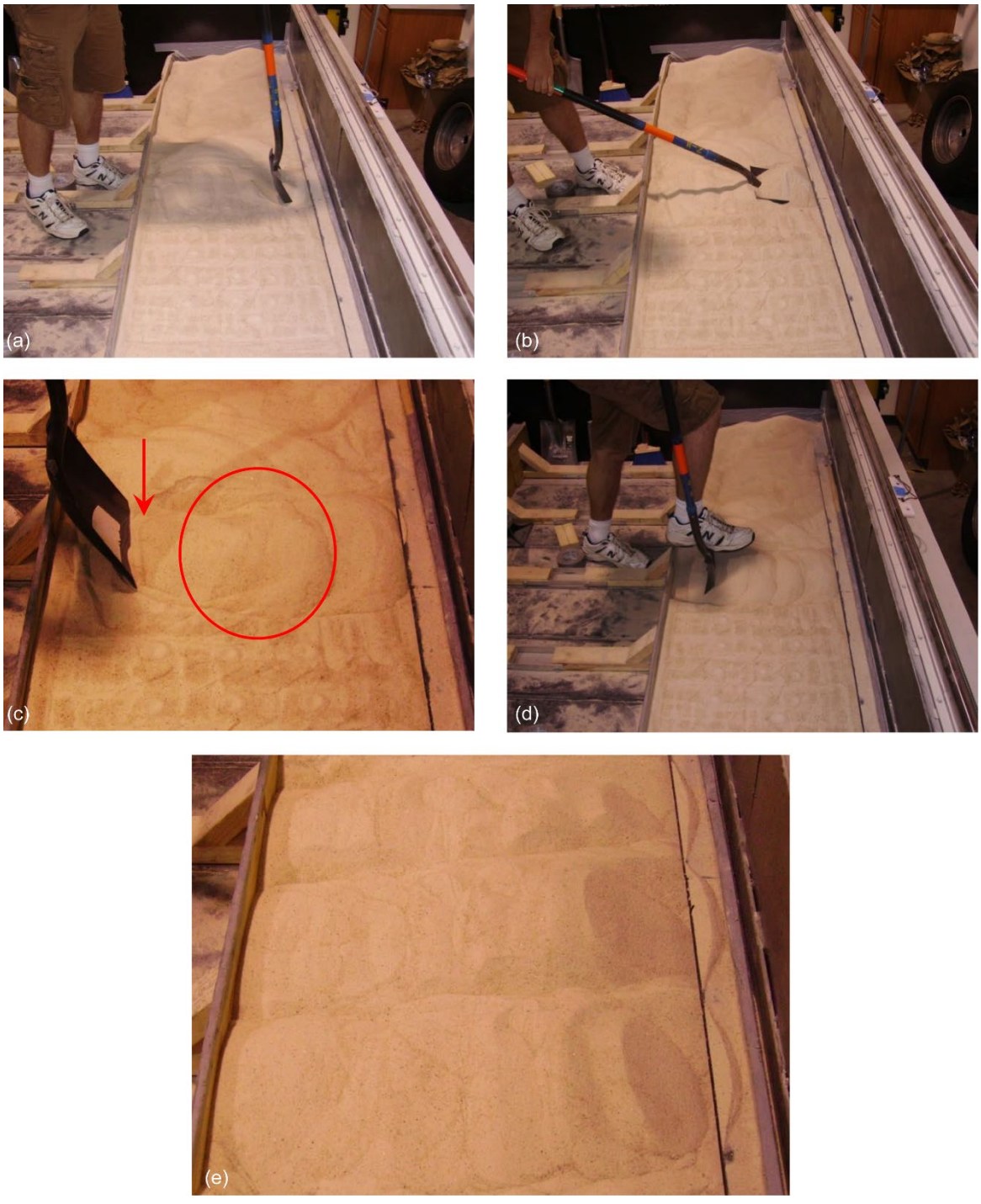

Figure 13.—Procedure for loosening the soil. (a) Step 1—Shovel inserted to bottom of soil bin. (b) Step 2—Shovel handle pulled back to lift soil. (c) Mound and valley pattern created by loosening technique. (d) Soil-loosening process repeated. (e) Testbed terrain after completion of the loosening process.

2.4.2 Leveling the Terrain

Leveling leads to a more even soil distribution; a flatter terrain surface; and in the case that the soil is compacted, creates a more even density. Creating a flat surface with even density results in less variation in the vehicle-terrain interactions. In addition, the flat surface may be used as a reference for measuring wheel sinkage.

(1) First, all major voids or valleys must be filled in. This is done by lightly running a rake through the track locations, eliminating major hills and valleys created by the loosening operation.

(2) Then, a leveling blade is pulled across the soil either manually or mechanically. In either technique it is important that the leveling blade does not rest on the soil itself, but is either suspended from above at a set height or supported by rails on either side of the soil bin. This prevents the soil from being compacted by the leveler itself.

2.4.3 Compacting the Terrain

The compaction stage of the soil preparation procedure provides control over the terrain density and resulting terrain strength. Two different compaction tools have been used at Glenn to produce different conditions: a tamper and a roller.

Tamper

- The tamper is a very good tool for accurately offsetting the terrain condition because the results may be varied based on the height at which it is dropped as well as the number of drops.
- Typically, an 8- by 8-in. (20.3- by 20.3-cm) tamper is dropped from about 8 to 15 cm above the surface in an overlapping pattern (about 50 percent for each pass) to make sure that the entire region is being compacted (see Figure 14). It is important to use only the weight of the tamper (4.5 kg), or possibly the tamper with a weight affixed to it, to apply pressure to the ground so that the procedure is user-independent.

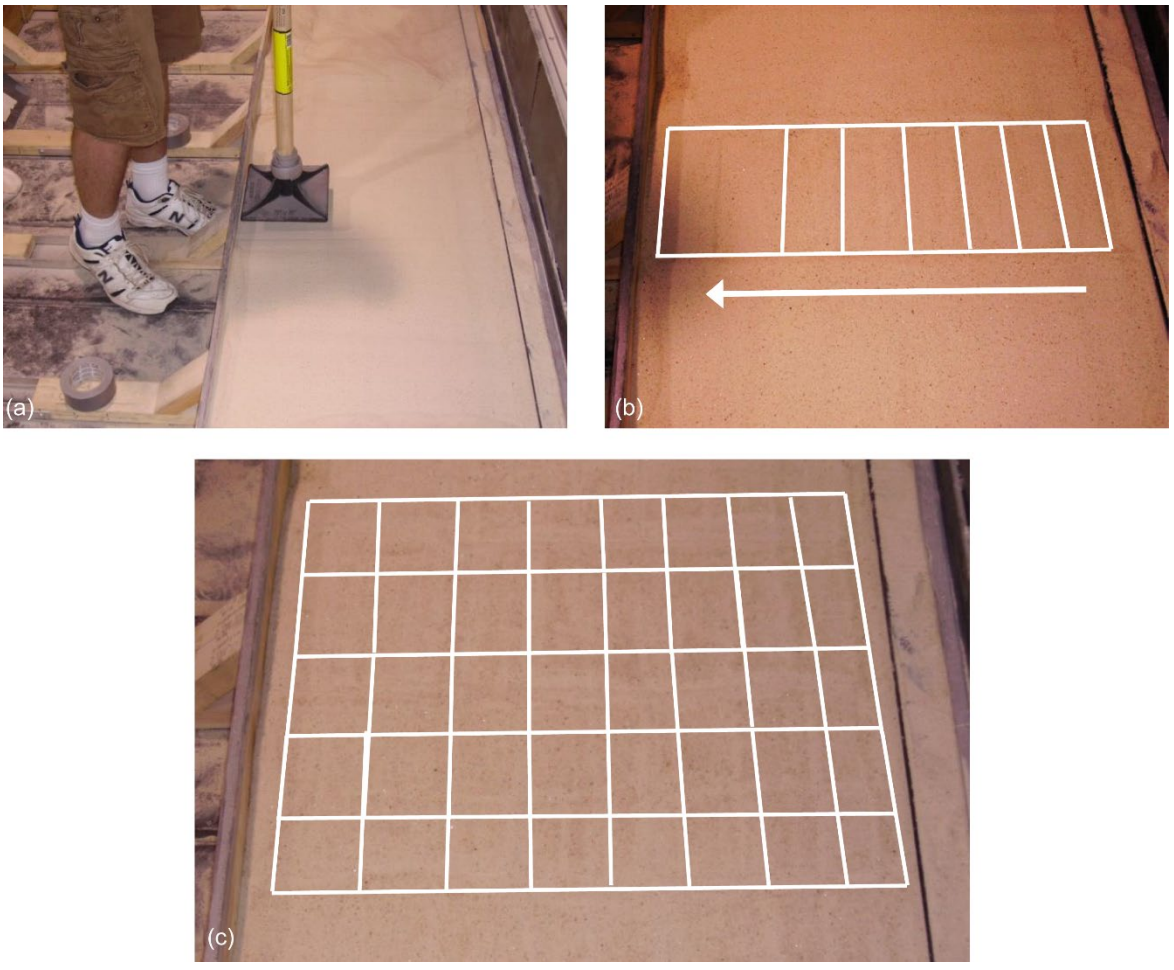

Figure 14.—Tamper compaction of soil. (a) Position of the tamper just before the operator released it. (b) Completed first pass. (c) Terrain compacted to a very dense condition.

Roller

- At Glenn, a standard 24-in.- (61-cm-) wide by 18-in.- (45.72-cm-) diameter lawn roller is also sometimes used to compact the terrain. Filling the roller with GRC–1, rather than water, adds additional mass (in this case 172.5 kg) for applying pressure to the ground. The roller is mechanically pulled by a winch at a constant rate along each of the wheel lanes, as shown in Figure 15.
- This method is very consistent and much quicker than the tamper method, but it does not allow for as much control over the terrain density. After the first pass, the measured cone index gradient did not increase appreciably, thus indicating that the density also was not affected much after the first pass.

Thus far, three primary terrain conditions have been created with the GRC–1 soil—each one using a combination of the loosening, leveling, and compacting methods just described. These three conditions were chosen on the basis of what could be achieved consistently and were intended to cover the range of cone index gradients that correspond to the Apollo 15 and 16 cone penetrometer data. The properties of each terrain condition are summarized in Figure 16 and Table IV.

Terrain condition T1: This condition is used to simulate lunar terrain that is on the high end in terms of density, with a target cone index gradient of 5.0 kPa/mm (see Figure 11). It is achieved by first loosening and leveling the terrain as described earlier. Then the 8- by 8-in. (4.5-kg) tamper is used by dropping it from a height of about 8 cm in rows that are perpendicular to the wheel track, where each row overlaps the previous by approximately 50 percent. A total of seven passes with the tamper are needed to create this condition.

Terrain condition T2: This condition falls in the lower range to midrange of densities observed on the Moon (Figure 11), with a target cone index gradient of 3.5 kPa/mm. The loosening and leveling steps are identical to those for T1, but the 24- by 18-in. roller filled with sand (weighing 172.5 kg) is used for compacting. This preparation is highly repeatable and much quicker than T1.

Terrain condition T3: The other major condition used at Glenn is a very loose state, aimed at replicating the most difficult traction challenge on the spectrum of lunar terrain conditions recorded. It is useful for testing because it provides very conservative predictions of vehicle performance on the lunar surface. Its target cone index gradient is 2.5 kPa/mm (Figure 11). For this condition, only the loosening and leveling stages of soil preparation are used.

2.5 Terrain Evaluation

For the reasons discussed earlier, the cone penetrometer was used to evaluate the consistency of these terrain conditions. The Rimik CP40II cone penetrometer (Rimik, 2015), which is similar to the standard WES cone penetrometer, was used in all tests at Glenn. The cone tip utilized had an apex angle of 30° and a base diameter of 20.3 mm (base area 323 mm^2), and it was mounted on a shaft with a diameter smaller than the base of the cone to reduce skin friction. The penetrometer was pushed into the soil manually, with the aim to achieve a constant velocity of 3 cm/s. Although the penetrometer measures penetration resistance continuously through 0 to 18 cm of depth, this particular device records only the average cone index gradient over 10-mm increments of depth. For example, over the first 10 mm of depth, the average penetration resistance was recorded and plotted at a depth of 5 mm. For these tests, zero depth was considered the point at which the base area of the cone was inserted flush with the soil surface.

The GRC–1 terrain preparation was evaluated on the basis of (1) the cone index gradient over a depth of 0 to 18 cm and (2) the homogeneity of the soil with depth (i.e., the linearity of the penetration-resistance-versus-depth curve). Again, the cone index gradient is defined as the ratio of the cone index to the depth of measurement in units of kilopascals per millimeters. Typically granular sand has a linear response to pressure over depth; therefore G was defined as the slope of the resulting cone-penetration-resistance-versus-depth curve. After the terrain was prepared for 4×4 vehicle tests, but prior to vehicle testing, the penetration resistance gradient was measured at eight places: four along the centerline of the right wheel track and four along the centerline of the left wheel track.

Figure 15.—Soil compacted with a 24-in. lawn roller pulled down the test lane via a mechanical winch.

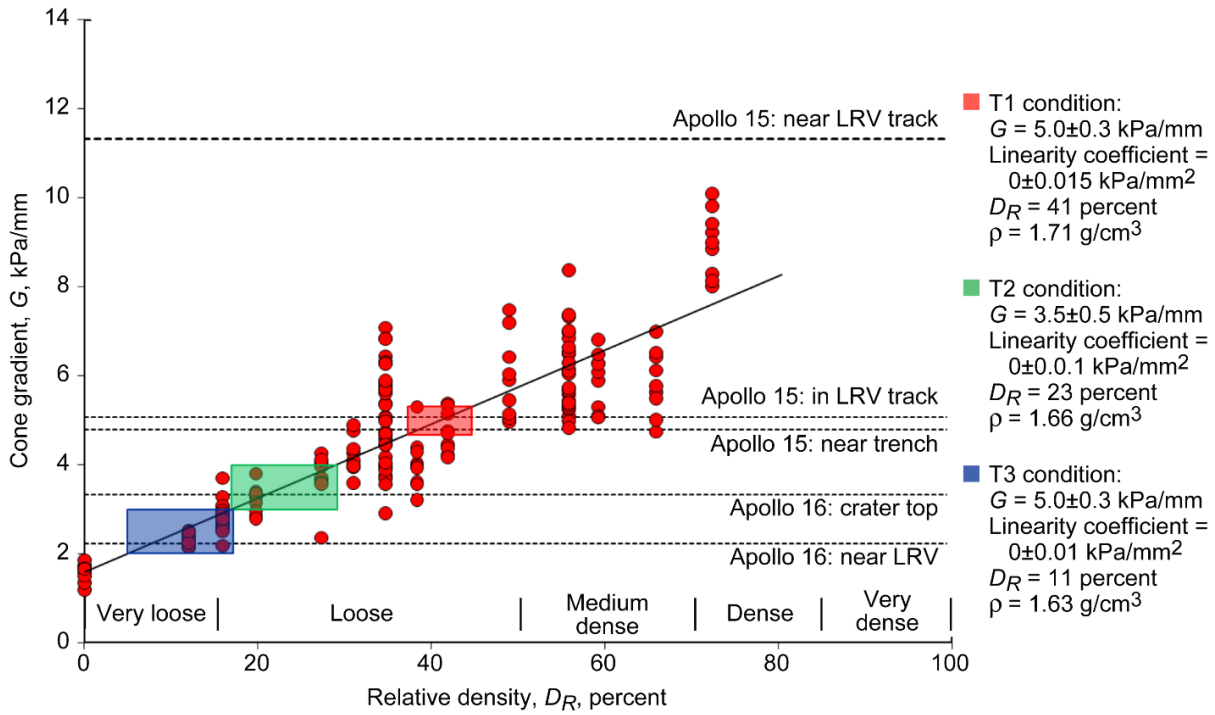

Figure 16.—Relationship between cone index gradient, G, and relative density, D_R, of Glenn Research Center 1 (GRC–1) for terrain conditions T1, T2, and T3. ρ = soil bulk density. Apollo data is represented along with a best fit line, $G = 0.0834(D_R) + 1.5811$.

TABLE IV.—TARGETED GLENN RESEARCH CENTER 1 (GRC–1) TERRAIN CONDITION (T1, T2, AND T3) PROPERTIES

Metric	T1	T2	T3
Target cone index gradient, kPa/mm	5.0±0.3	3.5±0.5	2.5±0.5
Standard deviation, kPa/mm	<1.0	<.5	< 0.5
Linearity coefficient, kPa/mm^2	0±0.015	0±0.01	0±0.01
Corresponding relative density, percent	~41	~23	~11
Corresponding actual density, g/cm^3	~1.71	~1.66	~1.63

For statistical evaluation, the result of each cone penetration test was plotted as a cone-penetration-resistance-versus-depth curve and the cone index gradient G was calculated for each data set by determining the slope of the linear regression line through the data points:

$$G = \frac{\sum_{i=1}^{k}\left(x_i - \bar{x}\right)\left(y_i - \bar{y}\right)}{\sum_{i=1}^{k}\left(x_i - \bar{x}\right)^2} \qquad (11)$$

where y_i is the value of a single cone index measurement in kilopascals with corresponding depth x_i in millimeters, $\bar{y}$ and $\bar{x}$ are the arithmetical mean penetration resistance in kilopascals and depth in millimeters, respectively, the index i is the test index, and the index k is the total number of observations in each data set.

The ensemble average of all eight cone-penetration-resistance-versus-depth curves was determined as well. A second-order polynomial was used to calculate a least-squares fit through the mean-penetration-resistance-versus-depth data points, providing a curvilinear trend as shown in Figure 7. The second-order coefficient, otherwise denoted as the linearity coefficient, was used to quantify the linearity of this curve; the closer it was to zero, the more linear the curve was. The linearity of the curve was equated with the uniformity of the soil preparation such that the more linear the curve, the more uniform the soil was with depth.

This method of terrain evaluation was applied to the three primary testing conditions: T1, T2, and T3. Data from Figure 10 were used to determine the relationship between cone index gradient and relative density for each condition; then the results were overlaid with the Apollo CPT data as shown in Figure 16.

Bulk density was interpolated using data from Oravec (2010). Table IV summarizes the three terrain conditions.

For perspective, the repeatability of the T2 terrain condition and WES's S2 terrain condition were compared. Both of the air-dry granular soils were prepared to these conditions in a similar fashion (i.e., loosening and compacting), and both provided mean cone index gradient values in the range of 3 to 4 kPa/mm. For this study, GRC–1 was prepared to the T2 conditions and 59 readings were taken over a variety of locations and preparations. The T2 condition produced a median gradient of 3.5 kPa/mm and a standard deviation of 0.2807 kPa/mm; by comparison, the WES S2 condition yielded a median gradient of 3.07 kPa/mm and a standard deviation of 0.2636 kPa/mm.

2.6 Terrain Preparation Conclusions

The following conclusions were based on the terrain preparation research:

(1) The cone index gradient *G* has been proven to correspond to bulk density for dry granular soils; therefore, it was chosen to be used as an indication of the state of the terrain. This value can also be mapped to other mechanical properties through empirical relationships.

(a) The cone index gradient also directly corresponds to vehicle mobility in dry granular soil (Green, 1967). This allows for vehicle performance to be predicted in a given soil on the basis of the *G* value.

(b) Because the cone penetrometer was used on the Moon, the lunar surface *G* values were used to establish lunarlike conditions with GRC–1 on Earth.

(2) The cone penetrometer can easily and quickly use the cone index gradient to verify the condition of the terrain. This is crucial both when methods to produce specific terrain conditions are being established and when the state of the terrain for vehicle tests is being checked.

(3) The lunar strength simulant GRC–1 was developed to reproduce lunar terrain-vehicle interaction under Earth ambient conditions. It can be conditioned to match the lunar terrain measurements over a range of bulk densities.

(4) Repeatable methods were established for each phase of terrain preparation: loosening, leveling, and compacting. Each of these methods involves basic terrain manipulation tools (shovels, tampers, etc.), but various combinations can be used to create different terrain conditions.

(a) Three easily repeatable terrain conditions for GRC–1 were produced using these methods: T1, T2, and T3. Each condition has a *G* value that falls within those measured on the lunar surface, with T1 being the firmest and T3 being the softest.

(b) The GRC–1 T2 condition was evaluated for its repeatability using the cone penetrometer. Fifty-nine readings were taken over a variety of locations and preparations; this resulted in a mean cone index gradient of 3.5 kPa/mm and a standard deviation of 0.2807 kPa/mm, indicating that the T2 preparation procedure is highly repeatable.

(c) Similar investigations should be performed for both the T1 and T3 soil conditions with a statistically significant data set.

(5) The current methods of soil preparation generally take about 20 min per testbed length (approximately 8 m) and are subject to slight changes because of variations in technique. The authors recommend that developing an automated method be investigated to decrease test preparation time and eliminate variations due to different personnel.

3.0 Analysis of Vehicle Test Methods

3.1 Test Vehicles and Configurations

In order to best characterize a specific tire design or vehicle configuration, it is important to perform DP tests under conditions similar to the application. These conditions can be defined by the terrain (discussed in Section 2.0), the externally applied forces, and the wheel control method (velocity-controlled, torque-controlled, towed, etc.). In the 1960s and 1970s, a variety of vehicle DP tests were performed at WES (Freitag et al., 1970; Turnage and Green, 1966). A simplified Jeep station wagon without a differential or suspension was used for a fundamental study on the reaction of soil under tire loads (Turnage and Green, 1966). Mass was added so that the weight would be distributed evenly. However, new test vehicles were built to simulate driving conditions on the Moon for an evaluation of the tractive capabilities of specific lunar tire designs (Freitag et al., 1970). These included a 6×6 Surveyor Lunar Roving Vehicle (SLRV) and a 4×4 test vehicle (Figure 17). These vehicles had very low mass, so the tire loads simulated what would be expected in lunar gravity (roughly one-sixth of Earth gravity). Another series of DP tests for lunar tires was conducted at the Yuma Proving Ground with a test vehicle called the Mobility Test Article GM–1 (MTA) (Northon, 1967). This vehicle was designed to represent the mobility system of the Lunar Mobile Laboratory (MOLAB) at one-fifth the mass (as close to lunar weight as possible).

At Glenn, two vehicles are currently used for DP tests, both having the capability to vary the tire load, wheel spacing, and center of mass. The Scarab rover (see Figure 18) was designed and built at Carnegie Mellon University (Wettergreen et al., 2010) under funding from NASA. It was constructed as a concept for an autonomous vehicle capable of traversing steep craters on the Moon in search of water. Scarab was then modified to be used for DP testing. This involved strengthening the chassis, modifying the wheel hubs for simple mounting of

various wheels, and adding mounts for weights at each wheel hub center so that a range of tire loads could be applied (approx. 980 to 2450 N per tire). The ability to apply a wide variety of loads to the tires enables the relationship between tire load and performance to be examined. It also allows for a range of tires to be tested with the same vehicle.

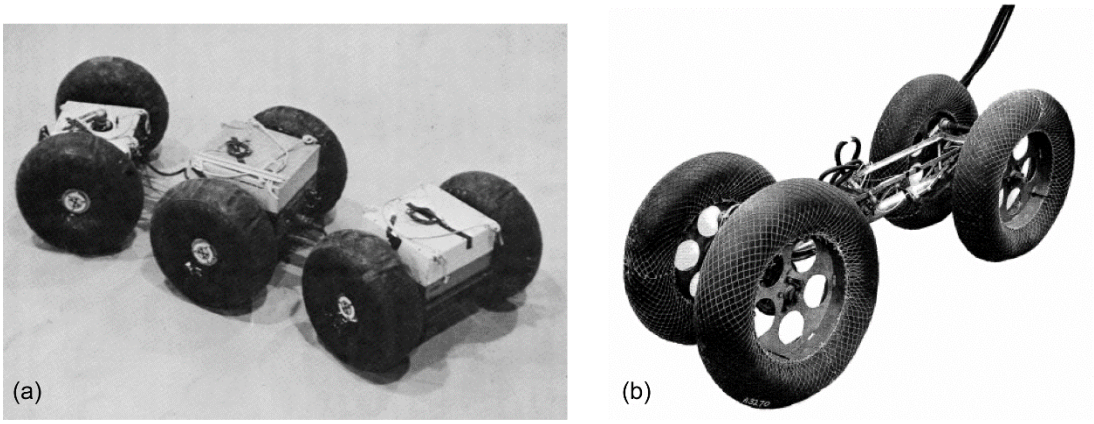

Figure 17.—Test vehicles for lunar simulations. (a) The 6×6 Surveyor Lunar Roving Vehicle (SLRV). (b) A 4×4 test vehicle used at the U.S. Army Waterways Experiment Station (Freitag et al., 1970).

Figure 18.—Scarab rover (Wettergreen et al., 2010), one of the vehicles used for drawbar pull (DP) testing at NASA Glenn Research Center.

Figure 19.—Glenn's dedicated tire test vehicle, Proteus, which was developed to simulate various driving configurations.

A dedicated tire test vehicle, Proteus, has also been developed at Glenn (Figure 19). This vehicle was built to be highly modular and versatile; it can establish not only a range of tire loads but also vehicle configurations. It can have four or six wheels, and the fore-aft position of each wheel can be adjusted easily. Each wheel module has independent steering and driving and can use a variety of steering methods (Ackerman, point-and-shoot, tank steering, radius turning, and turning in place). This vehicle can handle tire loads from approximately 590 to 1180 N; therefore, it can be used to test tires at lighter loads compared to Scarab, which is important when simulating driving conditions on the Moon.

3.2 Applying Drawbar Pull (DP) Force

3.2.1 Drawbar Pull (DP) Control Versus Velocity Control

There are two general methods for conducting DP tests: (1) the velocity of the vehicle (or rotational velocity of the wheels) must be controlled to create a known travel reduction, and the resultant DP force must be measured or (2) the force applied to the vehicle must be controlled, and the resultant travel reduction must be measured. At WES, the velocity of the vehicle was controlled through the use of a dynamometer carriage (Turnage and Green, 1966). The rotational velocity of the wheels on the vehicle was held constant, and the carriage, which was independently controlled and attached to the vehicle, was driven along rails at a commanded linear velocity. This velocity was varied to either hold constant or to ramp up the travel reduction of the vehicle. The force at the connection point between the vehicle and carriage was then recorded to get the DP force, F_{DP}. At the Yuma Proving Ground, a "Polecat" vehicle was used in a similar manner to induce travel reduction (Northon, 1967). The MTA was attached to this "slave" vehicle and then driven at constant wheel velocity. The velocity of the polecat vehicle was varied to induce travel reduction on the MTA, which resulted in changes to the DP force. Using a slave vehicle allows for test vehicles to be driven greater distances and in any environment, as well as in any direction. However, the mobility of the slave vehicle has an effect on the testing. For example, if the slave vehicle travels at an inconsistent rate (say due to changes in wheel slip), it will vary the travel reduction condition and resulting DP force applied to the test vehicle.

Alternatively, at Cranfield University's Off-Road Dynamics Facility (Brighton et al., 2006), a machine was used to apply a DP force to a full-size off-road vehicle and observe the travel reduction. Referred to as a "smart winch," this machine could feed a cable out under constant tension; thus the pull force on the vehicle could be controlled and its velocity could be measured. In the construction and industrial machining fields, the DP force is typically applied to the test vehicle using a "dynamometer car" (International Organization for Standardization, 1983). The dynamometer car is a machine towed by the test vehicle and controlled to maintain a constant resistance.

Both test methods (velocity controlled and force controlled) have been shown to yield similar results for a given wheel in a single-wheel test rig (Powell and Green, 1965). However, there are situations where this may not hold true, such as for a tire with widely spaced lugs. When the rotational velocity and linear velocity are controlled, the inconsistent radius length of the tire produces unintended variation in travel reduction. If the DP force were to be controlled instead, the vehicle velocity would account for these changes in radius. For vehicle testing, controlling the force applied to the vehicle is more natural and mimics what

occurs in normal driving. Travel reduction is generally a result of an outside force, not the controlled variable when driving. For these reasons, the testing at Glenn is force controlled.

It should be noted, however, that at higher force the performance of a vehicle is highly sensitive to small changes in the DP force (see Figure 20). Controlling the velocity instead of the pull force would allow for more high-end travel reduction values to be achieved. If it is important to populate this region of the curve, then the velocity-controlled method should be considered.

3.2.2 Drawbar Pull (DP) Rig

A DP rig was built (see Figure 21) at Glenn as a way to apply a controlled pull force on the test vehicles. The rig consists of an electric motor and a drum coupled through a magnetic clutch. A cable is wrapped around the drum and fed through a series of pulleys to a hitch on the vehicle. The torque on the drum is controlled through control of the current in the magnetic clutch, and the tension in the cable changes proportionally. This cable tension is what establishes DP force on the vehicle. Feedback from a load cell at the hitch point is

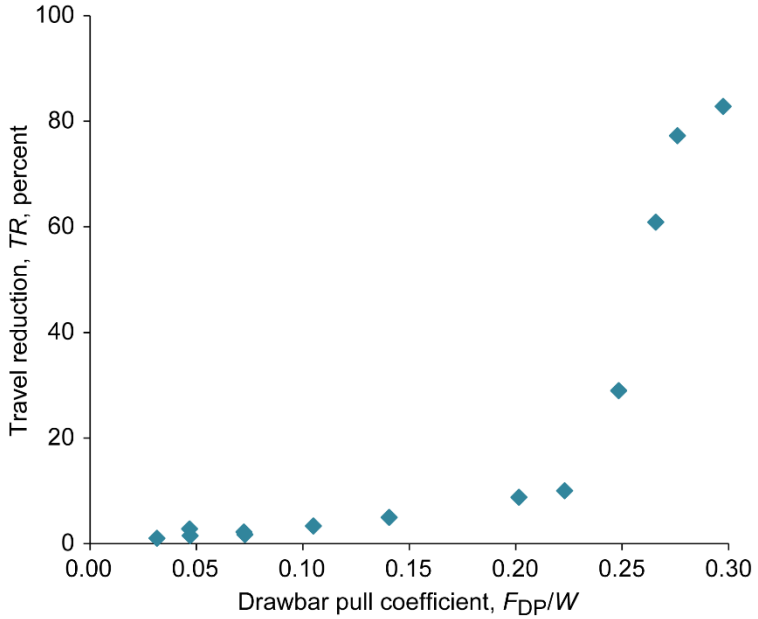

Figure 20.—Sample plot of drawbar pull (DP) force versus travel reduction.

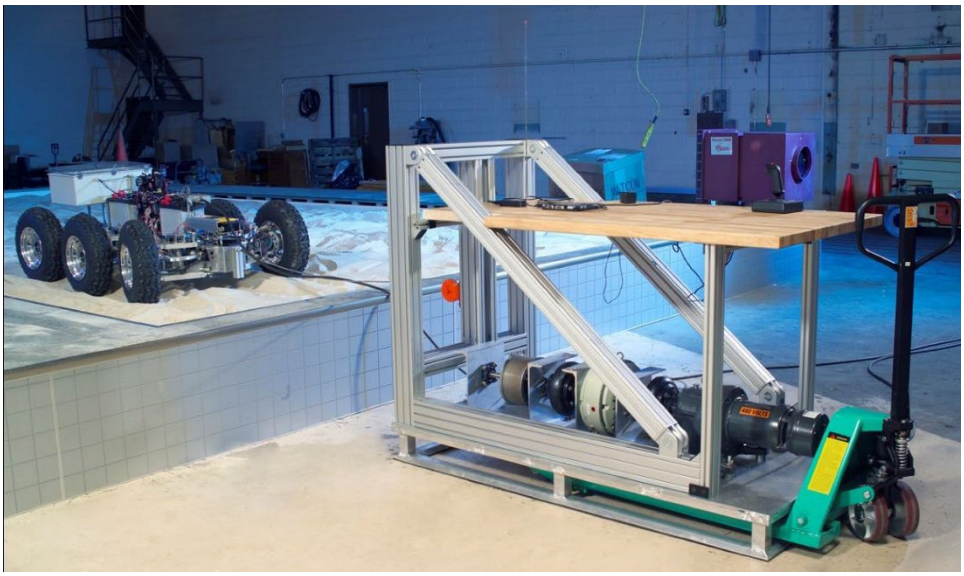

Figure 21.—Drawbar pull (DP) rig used to apply and control a pull force on a vehicle.

used to hold a constant DP force, F_{DP}, during a test or to vary the force as desired (such as in steps or at a constant rate of increase). The rig is mounted on an aluminum pallet, allowing it to be easily positioned throughout the lab.

3.2.3 Location of Hitch Point on Vehicle

From experience in Glenn's Simulated Lunar Operations (SLOPE) lab, it was found that the location of the drawbar hitch on the vehicle has an effect on the load distribution throughout the vehicle. The results from the DP test are simpler to interpret when the tire normal loads remain constant. However, as the DP force increases, so does the difference in the normal load between the front and rear axle, unless the hitch is at ground level. A study was conducted at WES (Turnage and Green, 1966) to understand the load transferred between axles at various DP forces F_{DP}. The 4×4 test vehicle was placed on two scales (one for each axle), and a range of F_{DP}'s were applied at the hitch height equal to one-seventh of its wheelbase. The relationship between DP force and change in load per axle was fairly linear; it was determined that the change in normal force on one axle was approximately 9 percent of the pull force. It is important to minimize this change in load as much as possible because the tire load is not generally measured during a test. This helps to reduce the effects unique to the vehicle (such as the suspension or wheelbase) so that tire performance can be compared across multiple test vehicles. In addition, DP test models lose accuracy if the load distribution is not taken into account. Because the normal load on each axle is typically not measured during a test, it is easiest to reduce the change in normal load as much as possible.

Figure 2 represents the forces acting upon a vehicle during a typical DP test (assuming rigid suspension).

A moment about the tire-terrain contact point of the rear tires (M_{rear}) was used to derive the following equations to obtain the normal load on the front axle (L_{front}):

$$\sum M_{rear} = 0 = Wx_{rear} - L_{front}\left(x_{rear} + x_{front}\right) - F_{DP}y_{DP} \qquad (12)$$

$$L_{front} = \frac{Wx_{rear} - F_{DP}y_{DP}}{x_{rear} + x_{front}} \qquad (13)$$

The moment about the contact point of the front tires (M_{front}) was then evaluated to obtain the load on the rear axle L_{rear}:

$$\sum M_{front} = 0 = -Wx_{front} + L_{rear}\left(x_{rear} + x_{front}\right) - F_{DP}y_{DP} \qquad (14)$$

$$L_{rear} = \frac{Wx_{front} + F_{DP}y_{DP}}{x_{rear} + x_{front}} \qquad (15)$$

The equations were then combined to find the difference in normal load between the rear and front axles:

$$\Delta L = L_{rear} - L_{front} = \frac{W(x_{front} - x_{rear}) + 2F_{DP}y_{DP}}{x_{rear} + x_{front}} \qquad (16)$$

It is clear that the closer the hitch point is to the ground, the less change will occur in tire load when the DP force is varied. If the vehicle's center of gravity is directly between the front and rear axle, the change in load is equal to the DP force multiplied by twice the ratio of hitch height to wheelbase. For this case, a theoretical plot of the relationship between hitch height and load transfer is shown in Figure 22. These data are for a vehicle driving under at F_{DP}/W = 0.2 with a center of gravity directly between the front and rear axles. Though putting the hitch at ground level may seem ideal, it is also important to keep in mind that as the vehicle pitches, or the tires sink or deform, the hitch point will drop as well. Thus, it is necessary to attach the DP cable at a point on the vehicle that will always stay above ground level. For testing with the Scarab rover, the load cell and DP cable were attached at the height of the wheel hub center, which was relatively close to the ground but always above ground level. This was achieved by wrapping ropes around the rear wheel hubs and attaching the cable to the center of a spreader bar between the two ropes (see Figure 23)—resulting in a hitch height of approximately 35 cm. Typically Scarab is driven with a wheelbase of 120 cm, thus the hitch height is equal to 29 percent of the wheelbase (see Figure 22). Of course this value will change with the tire size and wheel sinkage. Figure 24 shows the theoretical relationship between DP force and load transfer. This information can be used when modeling a DP test with Scarab. It also indicates that at high F_{DP}/W, the overall performance of the vehicle may be reduced slightly because the front tires are not providing the same amount of thrust as the rear tires.

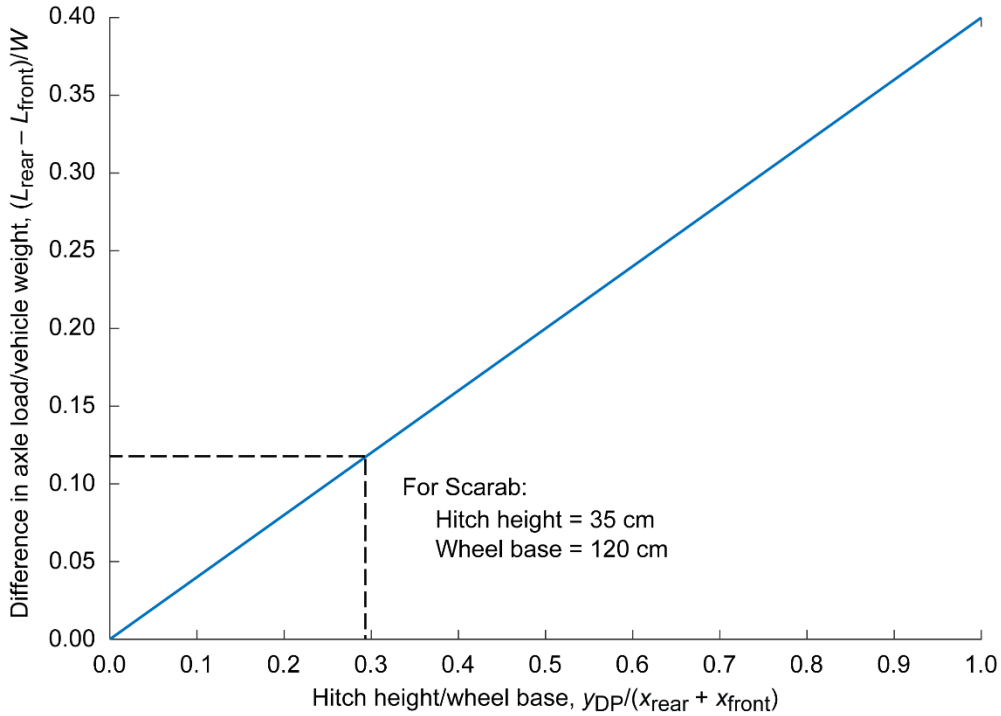

Figure 22.—Estimated effect of hitch height on load transfer at drawbar pull (DP) force coefficient F_{DP}/W = 0.2. (The center of gravity is centered between front and rear axles.)

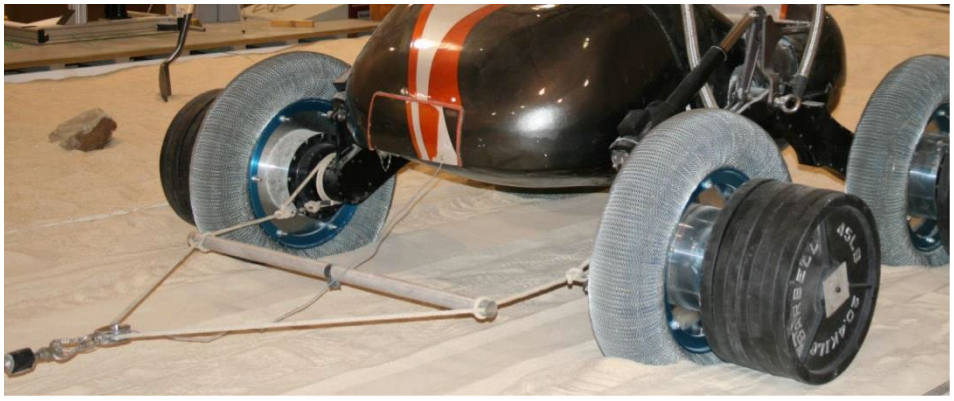

Figure 23.—Drawbar pull (DP) hitch attached at Scarab's wheel hubs.

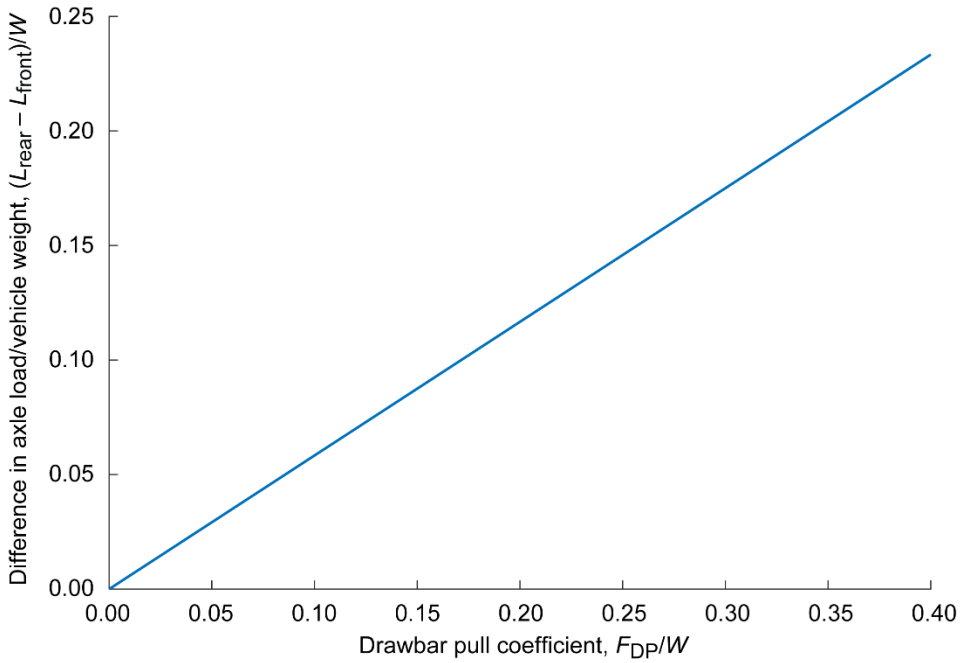

Figure 24.—Theoretical relationship between drawbar pull (DP) force, F_{DP}, and load transfer if hitch height is 29 percent of the wheelbase. (The center of gravity is centered between front and rear axles, assuming rigid suspension.)

TABLE V.—INTERVAL LENGTH OF EACH DRAWBAR PULL FORCE, F_{DP}, INCREMENT FOR RAMPED AND STEPPED F_{DP} METHODS
[Data were recorded only during the final 0.3 m of each stepped region.]

Method of applying F_{DP}	Distance between F_{DP} increments, m	Distance/tire diameter	Distance/wheelbase
Ramped F_{DP}, m	Constant increase at 62.3 N/m	----------	----------
Stepped F_{DP}, m	0.5	0.70	0.42
	.8	1.13	.67
	1.0	1.41	.83
	2.4	3.38	2.00
	4.8 (full length of bin)	6.76	4.00

3.2.4 Ramped Versus Stepped Increase in Force

During a test, DP force can be ramped up at a steady rate or increased in steps at varying distance intervals. Both techniques have advantages and drawbacks: ramping F_{DP} allows for a full F_{DP} versus *TR* curve to be completed in one run. However, it is more sensitive to error and to small variations in the terrain because each data point is taken at one instance or over a very small region, whereas with stepped drawbar tests, each data point is averaged over a large region, minimizing the effects of terrain variation or transducer error. The ramped DP force method also introduces acceleration, which can result in added inertial forces.

So that the effects of each method on a vehicle's performance could be evaluated, DP tests were conducted using both ramped and stepped DP force to compare travel reduction at various F_{DP}'s (Woodward, 2011). For the case where the force was increased in steps, the effect of the distance driven between each step also was studied. These distances ranged from 0.5 m (approximately 40 percent of the wheelbase) to 4.8 m (the full length of the testbed) (see Table V). In theory, the full-bin-length tests should produce the most accurate results because they best mimic a true steady-state condition in which a vehicle is driving on uniform terrain for an infinite distance.

For these tests, Scarab was driven with 71-cm-diameter, treadless pneumatic tires inflated to 30 psi and carrying a

980-N tire load (see Figure 25), and the soil was prepared to the T3 condition. Once the vehicle was driven into the prepared terrain, the DP force increased either in steps or at a constant rate. For the case of step increases, the load was increased at the specific distance intervals identified in Table V. Regardless of the interval length, the same DP forces were targeted for each test. For the stepped F_{DP} tests, data were averaged only over the final 0.3 m of each region. For the ramped F_{DP} tests, the F_{DP} and *TR* values were averaged over 0.05-m regions throughout the test. This distance was chosen because it represented a region over which the velocity could be considered constant but still allow for a decent sample size.

Figure 26 shows the results of these tests. The lines for the full-bin case (the most accurate but most time-consuming method), and the ramped case (the least reliable but fastest method) are, for the most part, very similar. In fact, there does not appear to be any consistent relationship between the increment distances and travel reduction. Because the ramped and stepped tests produced such similar results, it can be assumed that, at these slow velocities (35 cm/s), acceleration did not play a significant part in the vehicle's performance. These results indicate that DP force can be increased at a steady rate, rather than by step increases, to obtain reliable F_{DP} pull versus *TR* information.

Nevertheless, there are other benefits to using a stepped versus ramped F_{DP} technique:

- Specific wheel slip to travel reduction (*i* versus *TR*) conditions can be evaluated visually. For example, after a test, the tracks in the terrain can be analyzed and this knowledge can be used to predict vehicle performance in the field where little performance data are available.
- Specific cases (such as 0.2 F_{DP}/W) can be compared directly with various terrains or vehicle configurations.
- Wheel sinkage generally is not instantaneous, and it takes some time to either (1) reach a maximum depth for a given DP force or (2) obtain enough information to calculate a sinkage rate.
- Though the ramped force technique was proven to be accurate for this specific condition, it may not be as reliable for other terrains or vehicles.

For these reasons, the stepped F_{DP} technique was chosen as the standard method for DP testing at Glenn.

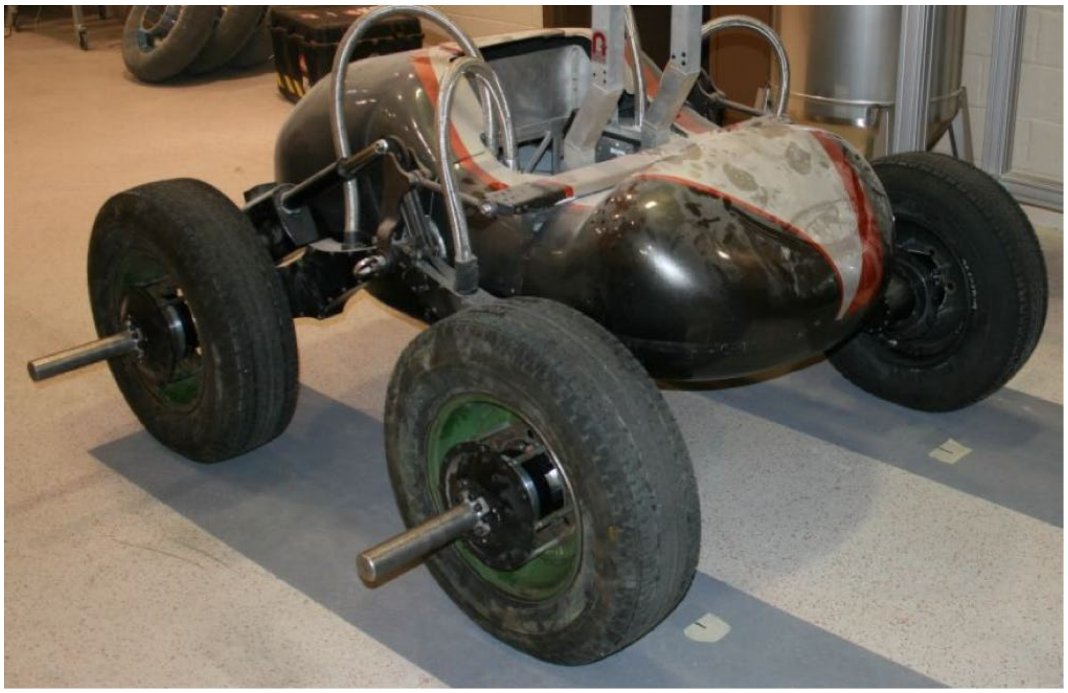

Figure 25.—Scarab rover with rubber treadless pneumatic tires.

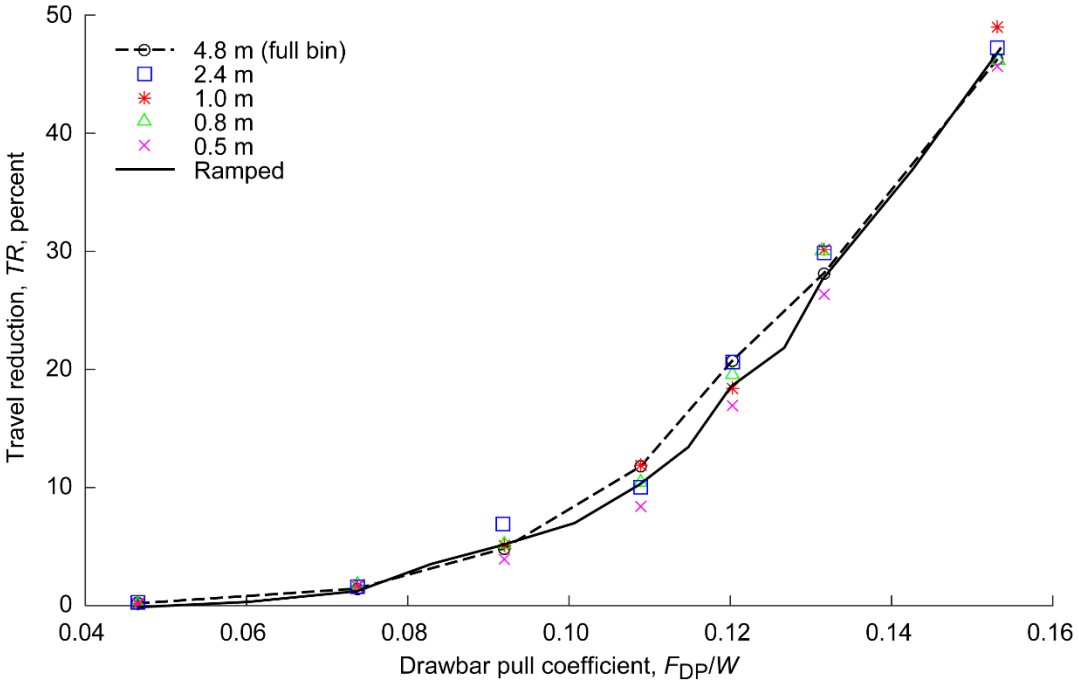

Figure 26.—Comparison of ramped and stepped drawbar pull force, F_{DP}, methods, showing F_{DP} versus travel reduction, *TR*.

3.2.5 Travel Length Required To Achieve Steady-State Condition

When stepped DP tests are being performed, there is the question of how far the vehicle must travel under each load before it reaches a steady-state condition—essentially, a point at which the performance no longer depends on distance. At WES (Turnage and Green, 1966), the test vehicle was driven two car lengths for each DP force applied, and only data from the second car length were used. This technique was assumed to create a somewhat steady-state condition because the rear tires would be driving in the ruts created by the front tires under the same load, simulating a vehicle driving an infinite distance.

The length increments listed in Table V were used to determine if a steady-state region could be achieved, in other words, a point at which the vehicle performance was no longer affected by the distance that it had traveled. It is important to note that, though these values represent the total distance that the vehicle drove under a specific load, only data from the final 0.3 m were used. For example, with the 2.4-m case, the vehicle drove 2.1 m, and then data were recorded for 0.3 m while the vehicle continued to drive before the F_{DP} was increased again. This choice of 0.3 m was used only for this study, so the samples sizes were consistent for the different methods. Typically, the data should be averaged over as large a region as possible, provided that the vehicle velocity and DP force appear to be constant.

From Figure 26, it appears that there is no obvious trend between step length sizes. So that this could be examined further, values were calculated for loads where all step length sizes were run; then these values were plotted as incremental length (or step length) versus travel reduction (Figure 27). For each load, there does seem to be a slight increase in *TR* from 0.5 to 0.8 m; though, after that, the performance does not follow any pattern. It is clear that after 0.8 m, the travel reduction does not depend on distance, indicating that either a steady-state region has been reached or the changes in terrain are insignificant to the vehicle's performance. It should be noted that these results are specific to this terrain condition.

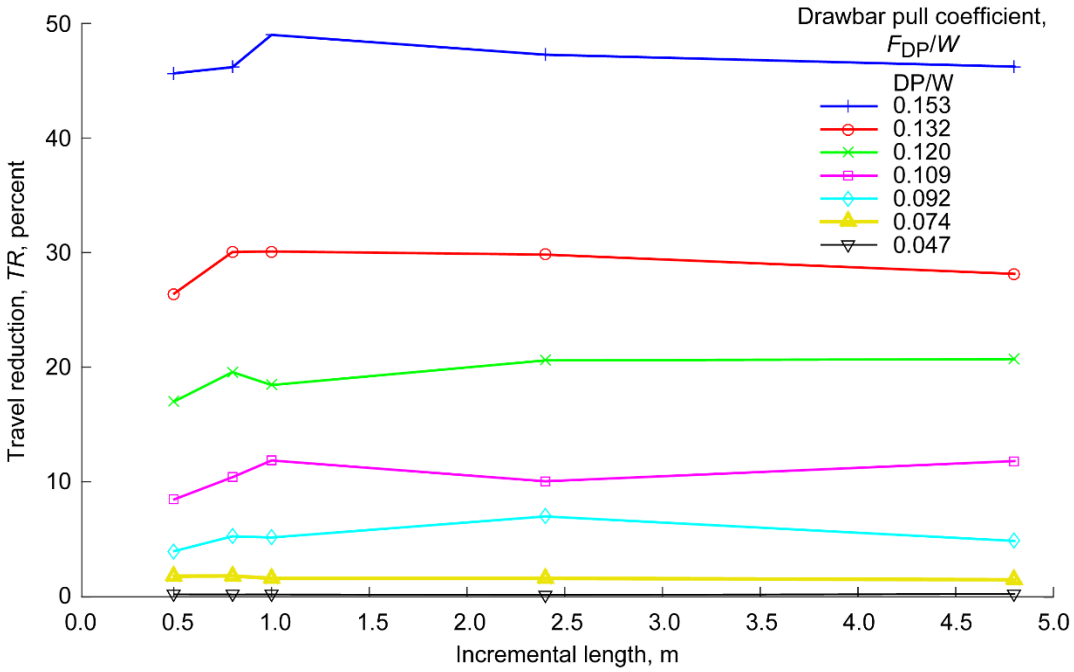

Figure 27.—Effect of distance traveled on vehicle performance for each drawbar pull (DP) region.

3.3 Method of Measuring Travel Reduction or Wheel Slip

The definitions of wheel slip i and travel reduction TR in Section 1.3.2 indicate that the method by which a reference velocity is measured has a significant effect on the results. Typically, a value for effective radius is determined ahead of time, using a designated zero-slip definition (Schreiber and Kutzbach, 2007). At the Yuma Proving Grounds (Northon, 1967), as well as in research performed by Wong et al. (1998), an extra towed wheel was used to obtain the reference velocity. For example, in a 4×4 configuration, an undriven fifth wheel would be attached to the chassis. Because vehicle velocity is equal to the radius of the towed wheel times its rotational velocity, the equation for wheel slip then becomes

$$i = \frac{r_r \omega_d - r_t \omega_t}{r_r \omega_d} \tag{17}$$

where

r_t radius of towed wheel, m

ω_d angular velocity of the driven wheels, rad/s

ω_t angular velocity of the towed wheels, rad/s

It is important to note that the towed wheel most likely has some negative slip (also referred to as “slide”) because of friction in the wheel module; thus this does not represent a zero-slip case. However, this can still be used as a reference velocity for calculating travel reduction.

Figure 28.—Robotic laser tracking system used to measure vehicle velocity.

At Glenn, this reference velocity is taken on a hard surface covered with a nonslip material. To compute vehicle velocity at Glenn, a robotic laser tracking station (Figure 28) is commonly used. A prism that is mounted to the vehicle reflects light along the same path that the light entered. When a laser is projected from the tracking station towards the prism, it is then directed back to the source and the time-lapsed images can be used to compute the distance between the prism and the tracking station.

The unit is also motorized, which allows the laser source and sensor to rotate about both a vertical and horizontal axis, tracking the vehicle throughout its path. The rotational movement data from the unit, combined with the distance measured from the laser, produce the three-dimensional coordinates of the vehicle with respect to time. These data can then be used to compute vehicle speed or distance traveled. The Scarab rover has encoders on its wheel motors, so wheel rotational data are logged directly from the vehicle's computer. Equation (6) is used to combine these parameters to obtain wheel slip *i* or travel reduction *TR*.

3.4 Measuring Wheel Sinkage

One generally either measures sinkage during a test by monitoring changes in the distance between the wheel hub and terrain surface (such as with laser range finders or the robotic tracking system) or assesses sinkage after a test by measuring the terrain rut depth. The former technique works best for stiff tires because changes in the tire deformation create measurement errors. The latter works best at low slip conditions because at high slip the tires can excavate soil that will backfill the ruts.

3.5 Use of Photogrammetry To Track Full Vehicle Motion

The techniques just described for finding vehicle velocity and sinkage, though accurate, are limited to tracking one point on the vehicle per sensor. Because the front tires generally undergo different sinkage than the rear tires, they require separate sensors. In addition, information on the rotation of the vehicle, such as pitch and roll, are not shown in these data sets.

A novel photogrammetry method was implemented at Glenn, which allows for the tracking of numerous points on the vehicle in three dimensions. A series of two-dimensional targets (in this case white circles) are placed strategically on one side of the vehicle, including on the chassis and the front and rear wheels (see Figure 29). Coded targets are also placed next to the bin to create a reference plane, and a pair of cameras are mounted at a distance that places the entire path of the vehicle in the field of view. Then while the vehicle is driven, the cameras are triggered synchronously at a constant rate. The photograph pairs are then uploaded to software called Pontos developed by Gom Optical Measuring Techniques (2013). Through a calibration procedure, the software is able to recognize the location and position of each camera relative to one another and therefore use the pixel location of the targets on the vehicle to determine their actual three-dimensional coordinates. When grouped together, these individual sets of coordinates are used to compute 6-degree-of-freedom motion for specific components on the vehicle, such as for one wheel. From these values, the velocity of the vehicle can be computed, as well as the vehicle's roll, pitch, and yaw. By measuring the vertical distance between the terrain surface and reference points outside of the bin, true sinkage can also be measured for rigid tires. If the tires are compliant, the sinkage can still be estimated using load-deflection data on the wheels (i.e., the deformed radius for a given load).

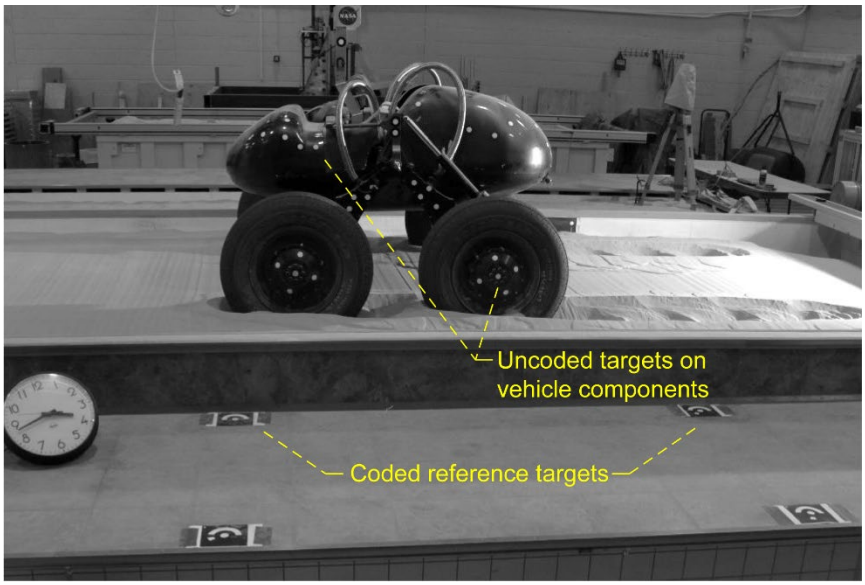

Figure 29.—Scarab with targets for photogrammetry tracking.

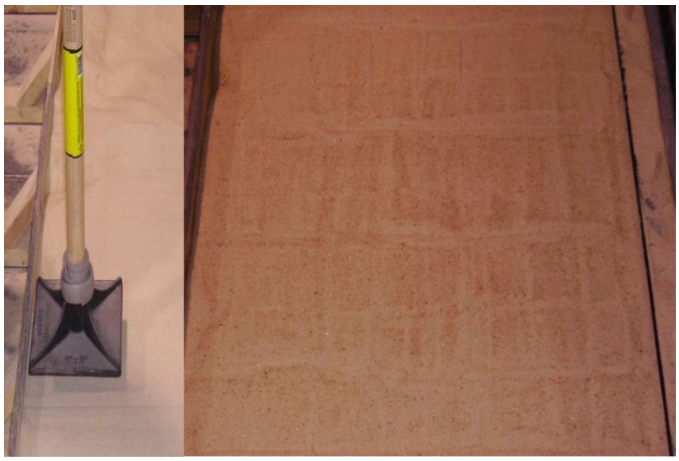

Figure 30.—Terrain compaction produced by dropping an 8- by 8-in. (20.3- by 20.3-cm) tamper from a specific height in an overlapping pattern (tamping method discussed in Section 2.4.2).

TABLE VI.—SUMMARY OF SOIL CONDITIONS TESTED
[Mean bulk density and mean relative density were interpolated using Figure 8 and Figure 9. Details on terrain conditions are in Section 2.5. Color bars correspond with color bars in Figure 32.]

Target cone index gradient, G, kPa/mm	Mean measured cone index gradient, G, kPa/mm	Corresponding mean bulk density, g/cm^3	Corresponding mean relative density, percent	Corresponding terrain condition
<2.0	1.86	1.61	2	
2.0 < G < 2.5	2.10	1.62	6	T3
2.5 < G < 3.0	2.70	1.64	13	
3.0 < G < 3.5	3.31	1.65	20	T2
3.5 < G < 4.0	3.78	1.67	26	
4.0 < G < 4.5	4.40	1.69	34	
>4.5	5.13	1.71	42	T1 (4.7 to 5.3 kPa/mm)

3.6 Effect of Terrain Preparation on Test Results

One major aspect of DP testing that can have a significant impact on vehicle performance is the terrain condition. It is important to have procedures that not only create a condition similar to wherever the vehicle/tires are designed to travel but can produce repeatable results. In the SLOPE lab, GRC–1 soil is used for DP tests where lunarlike strength properties are required (see Sections 2.1 and 2.3). The density of the soil is changed to create a range of terrain strength conditions that fall within the range measured on the Moon's surface (Section 2.4.3). A study was performed to understand how the vehicle's performance (in terms of travel reduction) is affected by this soil density variation.

As mentioned in Section 2.4.3, tamping provides a high degree of control and permits a wide range of variation in soil density. For this study, an 8- by-8 in. (20.3- by 20.3-cm) tamper with a mass of 4.5 kg was used to compact the soil (Figure 30). Density was controlled by varying the height at which the tamper was dropped and the number of drops in one spot. For all cases, the soil was loosened and leveled using the procedure described in Section 2.4. For the loosest condition (T3), no compacting took place; whereas for the rest of the conditions, various levels of tamping were used. Seven different soil conditions were created and tested, and the cone index gradient G was used as the metric for comparison. Table VI lists the seven conditions targeted, along with the mean cone index gradient measured and the corresponding density for each condition. The densities were estimated from data on GRC–1

that correlates bulk density and cone penetrometer gradient (Oravec et al., 2010).

For each of the conditions listed in Table VI, a complete *TR* versus F_{DP} curve was produced using the following procedures and configuration: 30-psi treadless pneumatic tires driven on Scarab with a tire load of 980 N, increasing the DP force every 0.5 m. A relatively high tire pressure was used so that slip and sinkage would be high and correspondingly the variations due to soil response would be emphasized. Again, only data from the last 0.3 m of each region were used to calculate an average F_{DP} and *TR*. The same values of F_{DP} were used for each soil condition for direct comparison. The results of these seven tests can be seen in Figure 31. It is obvious from this plot that aside from the three loosest conditions (*G* = 1.86 to 2.70 kPa/mm), there is a significant decrease in travel reduction as soil density increases.

So that the effect of soil density could be seen better, the data from these tests were also plotted as *G* versus *TR*, one curve for each F_{DP} (see Figure 32). There appears to be a consistent pattern for each F_{DP}; travel reduction is not sensitive to soil density until it reaches a condition represented by a gradient somewhere between 2.7 and 3.3 kPa/mm. Beyond this density, the travel reduction decreases steadily with cone index gradient (and thus soil density according to Figure 10) at a rate on the order of –5 percent/(kPa/mm). It should also be noted that at light DP load, the soil density does not have much impact on the performance above 4.4 kPa/mm. The T3 condition, which requires no compaction and has an average CPT gradient of 2.5 kPa/mm, falls within the region where small changes in soil density have very little impact on the vehicle's performance. Therefore, it was determined that the T3 condition is the most reliable condition for conducting DP tests. In addition, the T3 condition takes the least time to establish and is a relatively challenging condition for evaluating lunar mobility.

3.7 Verifying Repeatability of Test Procedures

In order to quantitatively evaluate the variability in the travel reduction data, a series of repeat tests were performed. Five tests were conducted at various levels of DP force to examine the range of variation. This range is a result of many factors such as differences in the soil density, ability to keep a constant DP force, and errors in data processing. The same tires and tire load described in the last section were used for this study.

The T3 condition was used for these tests because it was determined to be very repeatable and is commonly used for DP tests at Glenn. After the soil was prepared to this condition, the vehicle was driven out of the unprepared terrain with near zero applied F_{DP}. Once the back tires reached the prepared terrain, the F_{DP} was increased in steps every 0.5 m so that a full *TR* versus F_{DP} curve could be created in one run. This process was repeated five times, using the same set of DP forces each time.

The results of these five tests are shown in Figure 33(a). The values for F_{DP} and vehicle velocity were averaged over the last 0.3 m of each region to allow for the load to settle after each step increase. The residuals were calculated at each F_{DP} step using the following equation and are plotted in Figure 33(b).

$$r_n[F_{DP}] = TR_n[F_{DP}] - TR_{mean}[F_{DP}] \tag{18}$$

where

n	test number
$r_n[F_{DP}]$	residual in terms of *TR* for a given F_{DP} value and n, percent
$TR_n[F_{DP}]$	the measured *TR* for a given F_{DP} value and n, percent
$TR_{mean}[F_{DP}]$	the mean *TR* for a given F_{DP} value, percent

Standard deviation in travel reduction σ, was used to evaluate the repeatability of the test procedure. Using the equation below, values for standard deviation were computed at each F_{DP} step. The results are shown in Figure 34.

$$\sigma[F_{DP}] = \sqrt{\frac{1}{N}\sum_{n=1}^{N} r_n^2[F_{DP}]} \tag{19}$$

where

$\sigma[F_{DP}]$	standard deviation in terms of *TR* for a given F_{DP} value, percent
N	number of tests
n	test number
$r_n[F_{DP}]$	the *TR* residual for a given F_{DP} value and test number, percent

At the higher F_{DP} ranges, travel reduction becomes much more sensitive, and the resulting ensemble deviation increases to a maximum of 1.94 percent. However, even at the higher end, the values for standard deviation are relatively low considering that they are a combination of terrain variability, sensor error, and slight differences in the DP force. The authors concluded that these tests are in fact repeatable within a practical range of error.

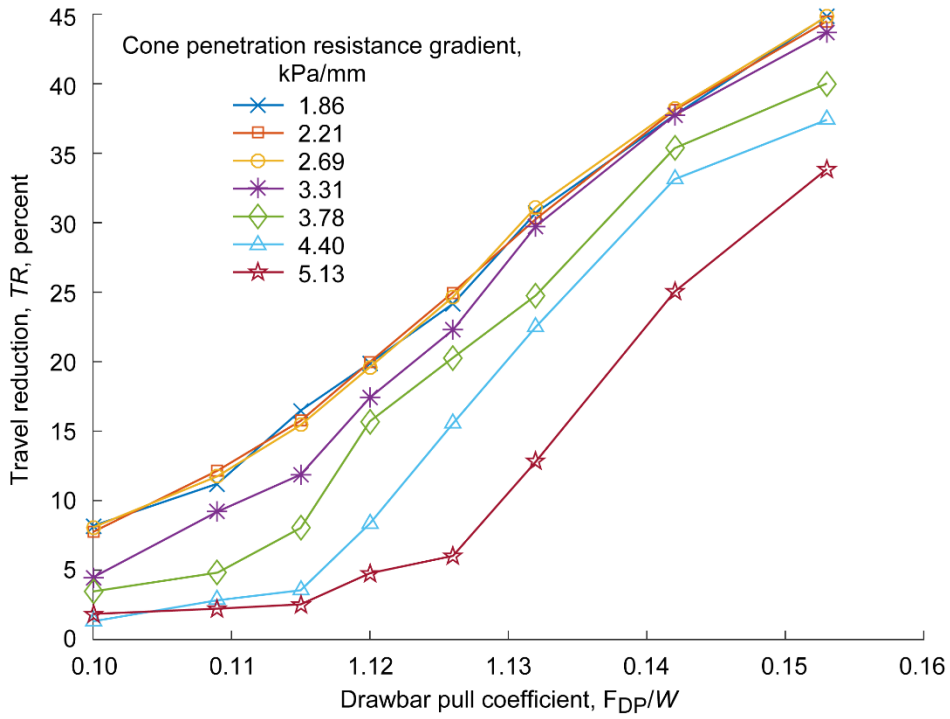

Figure 31.—Drawbar pull (DP) coefficient versus travel reduction for various soil conditions, identified by the mean cone index gradient.

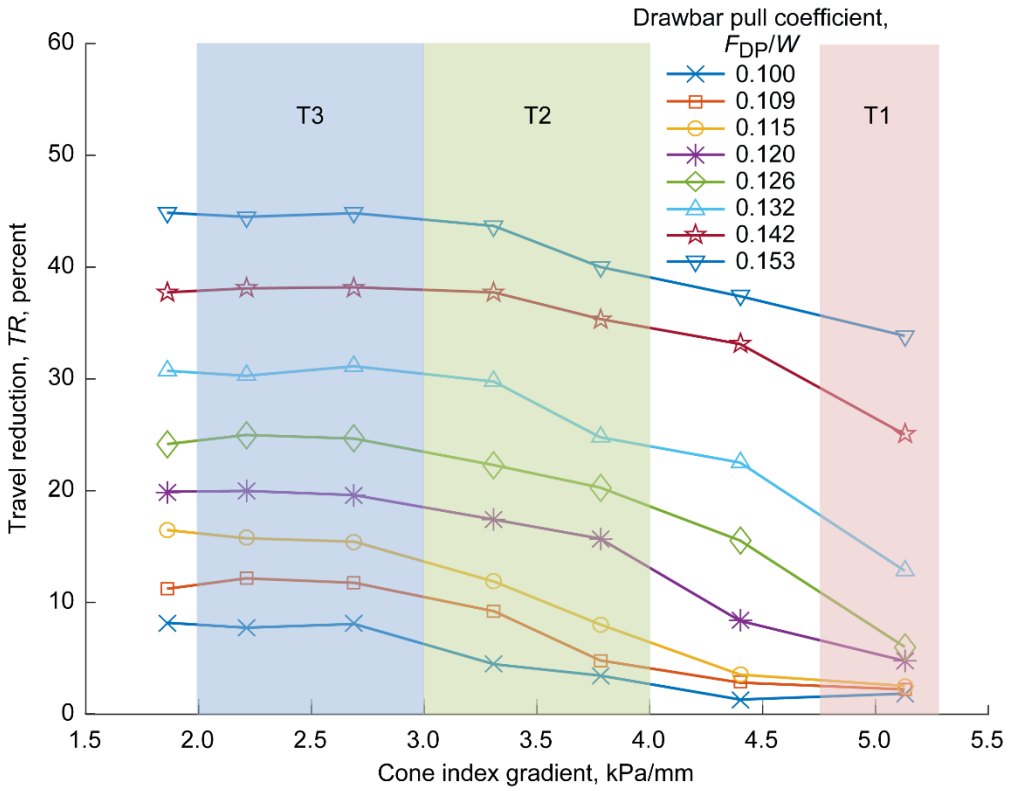

Figure 32.—Effects of soil condition (T1, T2, and T3), in terms of measured cone index gradient on vehicle performance under various drawbar pull (DP) forces.

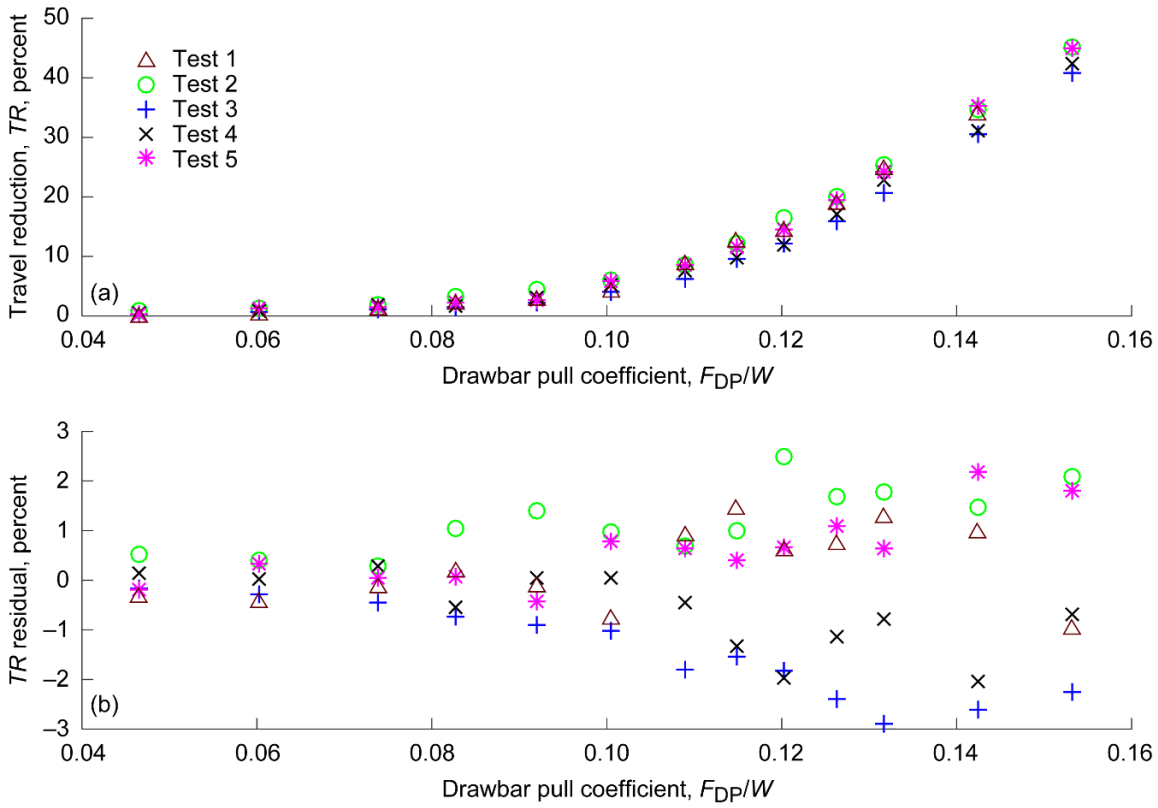

Figure 33.—Results of five repeat tests performed with 0.5-m increments in the T3 conditions. (a) F_{DP}/W versus *TR*. (b) *TR* residuals calculated at each value of drawbar pull coefficient, F_{DP}/W.

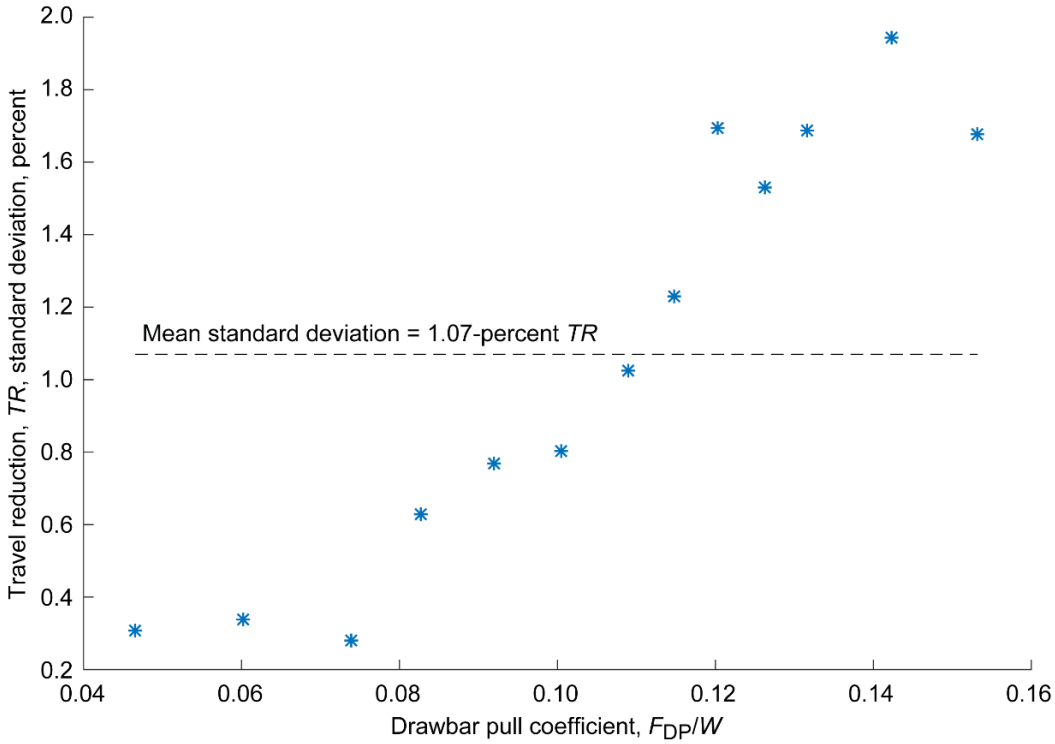

Figure 34.—Standard deviation for five tests plotted along a range of drawbar pull (DP) coefficients.

3.8 Vehicle Test Method Recommendations and Conclusions

From this analysis of vehicle drawbar pull (DP) test methods, the authors made the following recommendations and conclusions:

(1) When possible, a full-scale vehicle DP test should be conducted to evaluate the tractive performance of a wheel or vehicle. Though single-wheel tests are very good tools for comparing the relative performance of wheels, they do not take in to account differential loading and vehicle dynamic that occur in real-world operations.

(2) Further study should be conducted on the effects of controlling DP force versus controlling vehicle velocity. In theory, it is best to control the pull force because in typical driving scenarios, travel reduction (or wheel slip) depends on external forces and is not controlled. In addition, wheel slip is not always constant for a given DP force, such as in the case of a tire with widely spaced lugs. The difference in effective radius results in periodic slip. In this case it is not clear that constant velocity control would provide the same DP force/travel reduction, F_{DP}/TR, relationship as constant force control would.

It is important to collect enough data to complete a full *TR* versus F_{DP} curve rather than comparing the performance at only one or two discrete points. This is because the shape of the curve varies for different terrain and vehicle configurations, so the relative performance between two sets of wheels may be different at various points on the curve.

(3) It is important to understand the normal load distribution on each wheel throughout a DP test. This allows for individual wheel performance to be quantified and for accurate data comparison between different vehicles or laboratories.

(a) Knowing the normal load on each wheel is also useful for modeling the vehicle performance.

(b) To minimize the change in normal loading throughout a test, the pull force should be applied on the vehicle at a point near the terrain and the vehicle should be pulled in a horizontal direction.

(4) Further study should be conducted on the effects of ramped versus stepped F_{DP} control. NASA Glenn Research Center researchers determined that applying DP force in increasing steps is ideal because it allows the wheels to reach a steady-state condition (i.e., no trending change in F_{DP} or *TR* after this point). It also allows for comparison of performance at specific F_{DP} values. However, it is much more time-consuming than conducting a ramped F_{DP} test.

For the test conditions discussed here, a step length of 0.8 m was sufficient for each increase in F_{DP} when tires with a diameter of 0.71 m and a wheelbase of 1.2 m were used. However, this depended on wheel size and wheelbase. Researchers should either be conservative in the choice of step size or conduct a study similar to the one described here to determine the distance needed to achieve steady-state conditions.

(5) Wheel slip and travel reduction are excellent metrics for understanding the relative tractive performance and efficiency of various wheels or vehicles. However, wheel sinkage (relative to wheel radius) should be used to indicate the likelihood of immobilization. It is important to quantify this for each wheel, not just the system as a whole, since the sinkage will likely be different at each axle.

(6) Vehicle performance is highly sensitive to terrain condition. It is important to use a method of preparing the terrain that results in conditions that are consistent from test to test. At Glenn, this is done by first loosening the soil with shovels, leveling it with a blade, and then (if desired) compacting the terrain with either a tamper or roller. The terrain condition varied the least when the soil was not compacted (the T3 condition).

(a) The terrain condition should be measured with a cone penetrometer before each test to verify that the cone index gradient falls within the specified range. This information can also be correlated with soil density.

(b) The methods used at Glenn all rely on human interaction, but an automated method of loosening, leveling, and compacting the soil would be ideal. This would remove user error and would likely save time.

(7) The vehicle DP test procedures used at Glenn were determined to be highly repeatable. If significant changes to the procedure are made (such as a new terrain preparation method), the repeatability of the new procedures should be verified by running at least five identical tests and statistically comparing the results.

Glenn Research Center
National Aeronautics and Space Administration
Cleveland, Ohio, August 31, 2017

Appendix A.—Symbols

a	vehicle acceleration, m/s^2
CI	cone index
D	soil density, percent
d	distance traveled, m
E	total energy consumption, J
F	force, N
F_{DP}/W	drawbar pull coefficient (drawbar pull force normalized to vehicle weight)
G	cone index gradient (cone penetration resistance gradient), kPa/mm
i	slip, percent
k	number of data points
L	normal load, N
M	moment about tire-terrain contact
m	vehicle mass, kg
N	number of tests
n	test number
P	total power consumption, W
PN	power number
R	resistance, N
r	radius of wheel, m (Eq. (17))
TR	travel reduction, percent
v	forward velocity of vehicle or wheel axle, m/s
W	vehicle weight, N
x	depth, mm
$\overline{x}$	arithmetic mean depth, mm
y	cone index (cone penetration resistance)
$\overline{y}$	arithmetic mean cone index, kPa
z	wheel sinkage, cm
η	tractive efficiency (drawbar efficiency)
ρ	soil bulk density, g/cm^3
θ	angular rotation of each individual wheel
σ	standard deviation in terms of travel reduction, percent
ω	angular velocity of wheel, rad/s

Subscripts

axles	both axles
CG	center of gravity
d	driven
DP	drawbar pull
front	front wheel or axle
i	text index
mean	mean value
n	number of observations in each test set
R	relative
r	rolling (effective)
rear	rear wheel or axle
ref	reference condition
t	towed

Appendix B.—Procedures Used for Drawbar Pull (DP) Testing at NASA Glenn Research Center

B.1 Data Acquisition Equipment

(1) A total station is used to record vehicle velocity.

(a) Make sure that the prism is mounted firmly on the vehicle and is within clear view of the total station.

(b) Make sure that the total station is calibrated and properly leveled.

(2) Photogrammetry equipment (cameras and targets) are used to track wheel sinkage (see Section 3.4).

(a) Calibrate the system using the manufacturer's procedure every time the camera orientation is changed.

(b) Make sure that all targets on the vehicle and wheels, as well as reference targets, are in view of both cameras before each test.

(3) The computer on the vehicle logs wheel rotational velocity and wheel torque.

The data logger must be restarted remotely before and after each test.

(4) The computer on the DP rig logs the DP force.

B.2 Rolling Radius Measurements

Any time that the vehicle configuration changes (e.g., new tires, tire pressure, or vehicle weight distribution), the rolling radius should be measured as follows. Summarize these results using the "vehicle/tire configuration" data sheet shown in Figure 35.

(1) Using floor scales under each tire, set the weight distribution to achieve the desired tire loads.

(2) Place the vehicle on hard ground that is covered with anti-slip tape.

(3) Drive the vehicle forward at least one full wheel rotation and measure the total distance traveled d as well as the total angular rotation of each individual wheel θ.

(a) Log the angular rotation of each wheel using the wheel encoders on the vehicle.

(b) Mark the start and end positions of each wheel on the ground and measure the linear distance traveled of each with a tape measure.

(c) It is important to note that the wheels may not all turn the same amount, so each one should be measured independently.

(4) Calculate rolling radius r_r.

$$r_r = \frac{d}{\theta}$$

(5) Repeat steps (1) to (4) (at least two times), and compute the mean rolling radius for each tire.

B.3 Soil Preparation

(1) Drive the vehicle to its starting position at one end of the test lane.

(2) Determine the desired terrain condition and prepare it using the methods discussed in Section 2.4.

(a) Loosen the soil to return it to its original state.

(b) Level the terrain.

(c) Compact the terrain as desired.

(3) Take eight readings with a cone penetrometer in the intended tire tracks. Space these throughout the length of expected vehicle travel, taking four readings down the middle of each tire track.

(4) Using the methods described in Part 2, Terrain Evaluation, calculate the cone index gradient G, standard deviation, and linearity coefficient, and verify that they are within the desired range of values (see Eq. (11), Figure 7, and Table IV).

Log the CPT file and cone index gradient on the DP test data sheet in Figure 35.

B.4 Drawbar Pull (DP) Test

Use the DP test data sheet (Appendix C) before and during each test to note the important test parameters.

(1) Attach the cable from the DP rig to a hitch point on the vehicle.

(a) As discussed in Section 3.2.3, it should be as close to the ground as possible without touching the surface at high slip. It should also pull evenly on both the right and left sides of the vehicle.

(b) For Scarab, the hitch point is established by wrapping cables around the rear wheel hubs and using a spreader bar to keep the pulling forces on each side of the vehicle parallel.

(c) The hitch height relative to the wheelbase distance should be noted on Figure 35.

(2) Apply just enough DP force with the DP rig so that the cable does not rest on the ground.

(3) Start the DP rig program (commands rig to increase the cable tension at desired increments and distances).

(4) Begin logging data.

(5) Drive the vehicle at a constant wheel rotational velocity.

The vehicle should be driven at least the length of one wheelbase (distance from the front to back axle) so that the rear

tires are driving in the ruts of the front tires. Data collected prior to this condition should be considered invalid.

(6) Increase the DP force in steps with consistent lengths of travel distance.

For the case discussed in Section 3.2.5, a distance of 0.8 m was found to be the minimum needed to achieve steady-state conditions for 0.71-m-diameter tires with a wheelbase of 1.2 m. This can be used as a basis for determining the appropriate travel distance.

(7) Once the vehicle has reached the end of the prepared testbed, stop the vehicle, stop the DP rig program, and stop recording data.

(8) Compute the average F_{DP}, torque, vehicle velocity, and wheel rotation velocity for each DP step.

(a) In each step, use only the data for which the DP force appears to be constant (see Figure 36, Appendix D for an example of raw data). This is to eliminate any effects of vehicle acceleration or settling of the DP force feedback control.

(b) Use the point at which the vehicle begins to move to synchronize data from the various sources.

(c) Divide each average F_{DP} value by vehicle weight to get F_{DP}/W.

(d) Compute mean travel reduction at each F_{DP} using Equation (6).

(e) Compute power number and tractive efficiency at each F_{DP} step using Equations (8) and (10).

(9) Use the photogrammetry data to compute sinkage at each F_{DP} step (see Section 3.4).

Use the change in time from when the vehicle started to move to identify the appropriate photogrammetry stage to use for each F_{DP} step.

(10) The DP test procedure should be repeated as needed to obtain a complete F_{DP}/W versus TR curve (see Figure 37 and Figure 38).

(a) This typically requires 8 to 12 F_{DP}/W values.

(b) Plot the power number, tractive efficiency, and sinkage as a function of F_{DP}/W (see Figure 37 and Figure 38).

Appendix C.—Sample Data Sheets

VEHICLE/TIRE CONFIGURATION

Tire type:

Nominal tire load = Nominal diameter =

Tire #	Serial/ID #	Effective Radius	Tire Load
Front Left			
Front Right			
Rear Left			
Rear Right			

Mean Eff. Radius =

Vehicle Load =

Front Axle	
Load	
Height	
X-coord.	0 cm
Track Width	
Driven?	

Rear Axle	
Load	
Height	
X-coord.	
Track Width	
Driven?	

Hitch	
Height off terrain	
X-coord.	

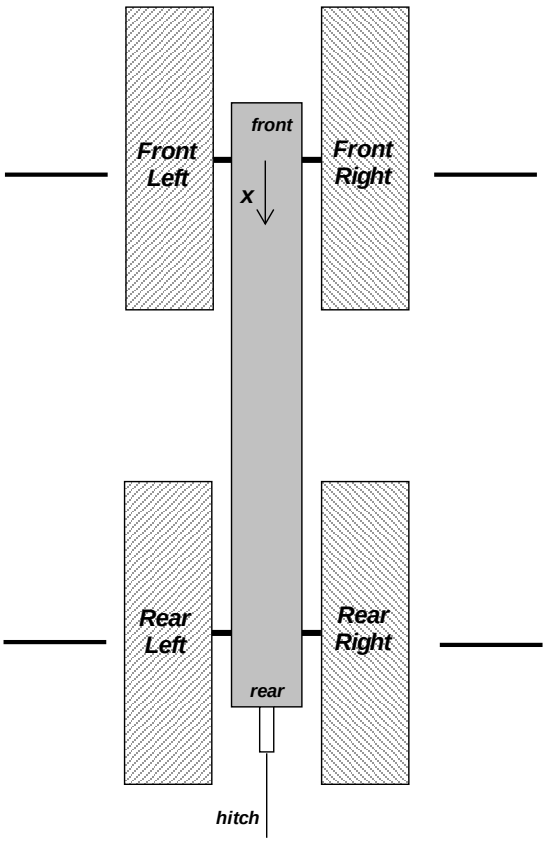

NOTES:

Figure 35.—Drawbar pull (DP) test data sheets.

DRAWBAR PULL TEST

Test #: **Date:**

Tire type:

Tire load = Nominal diameter =

Room temperature = Room humidity =

Soil condition:

CPT File #: CPT Gradient =

Telemetry File:

Scarab Data File:

Region #	DP Motor Current (A)	DP force, F_{DP} (lbs)	Start Time (s)	End Time (s)

Figure 35.—Concluded.

Appendix D.—Sample Drawbar Pull (DP) Test Data

Figure 36 is a sample plot of data collected during a DP test. This particular test is for a vehicle with 71-cm-diameter tires and a 980-N tire load. There are four usable regions where performance metrics can be calculated here. Note that the vehicle begins driving after around 60 s.

By averaging the wheel rotational velocity, vehicle velocity, DP force, and torque in each of these regions, the performance metrics can be calculated and plotted, as shown in Figure 37.

After enough tests have been run to cover the necessary range of F_{DP}/W values, complete data sets can be plotted together. Figure 38 shows a complete set of performance metrics for this specific vehicle/tire configuration. Tractive efficiency is represented in Figure 39. Sinkage is not included here because the current procedure for computing sinkage had not been implemented when this test was conducted.

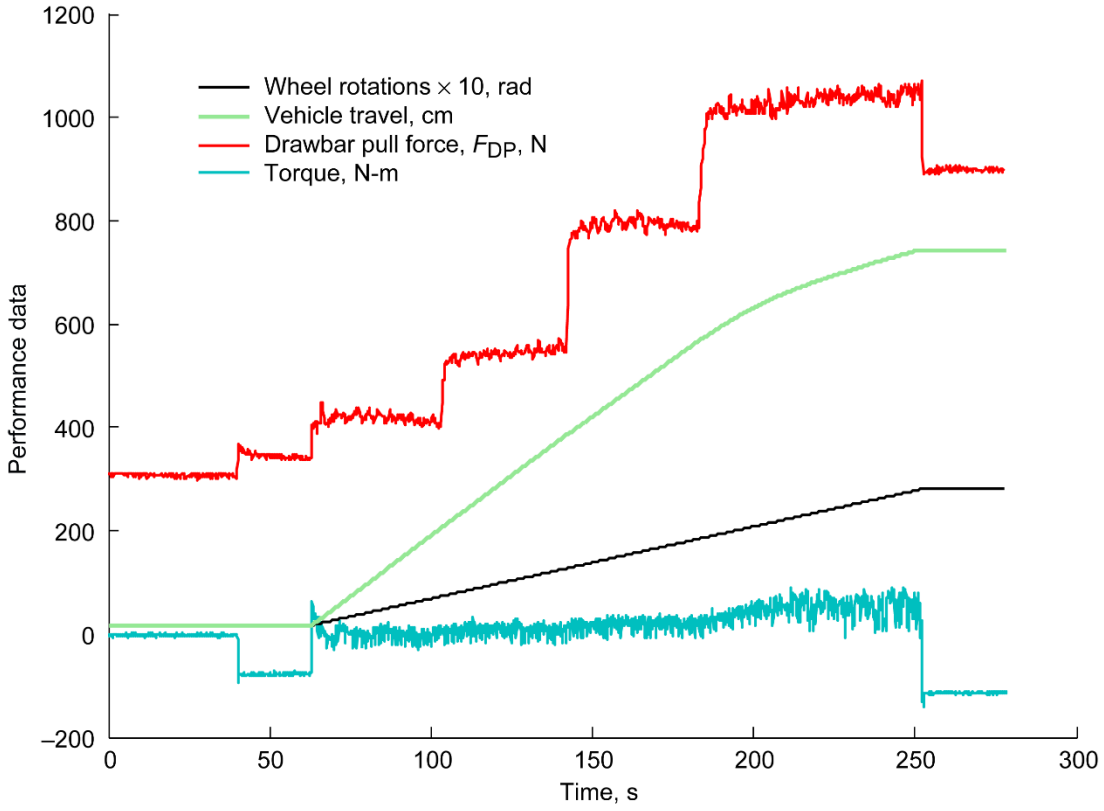

Figure 36.—Sample raw data plots (wheel rotation has been scaled ×10 for visibility).

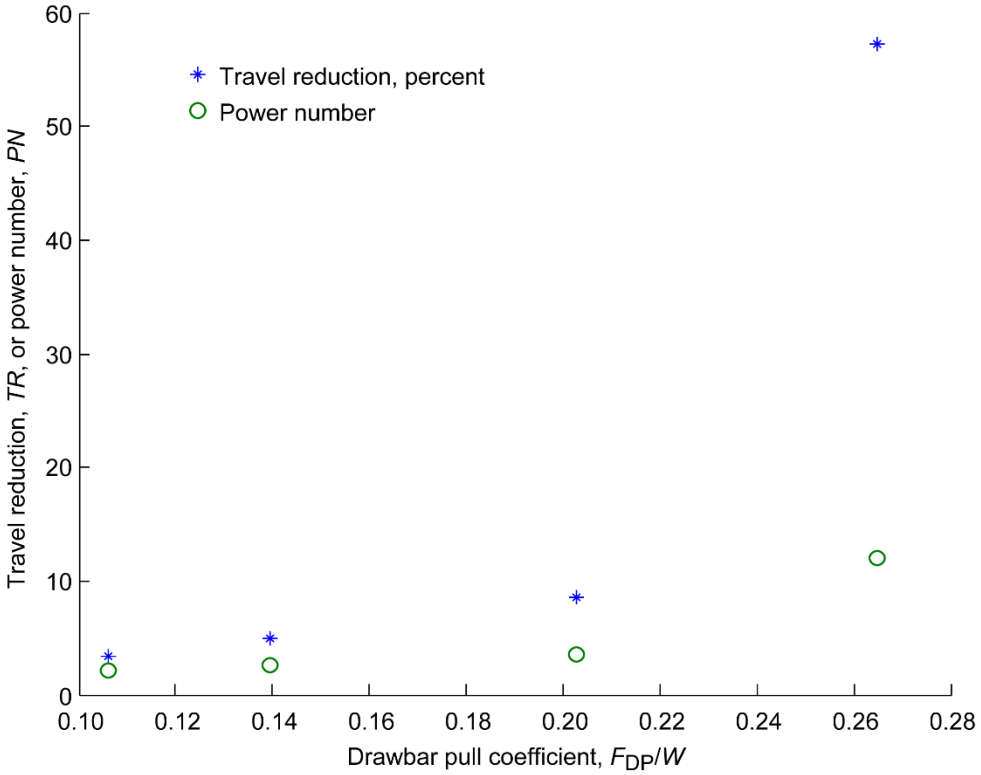

Figure 37.—Travel reduction and power number versus drawbar pull (DP) coefficient for one test run.

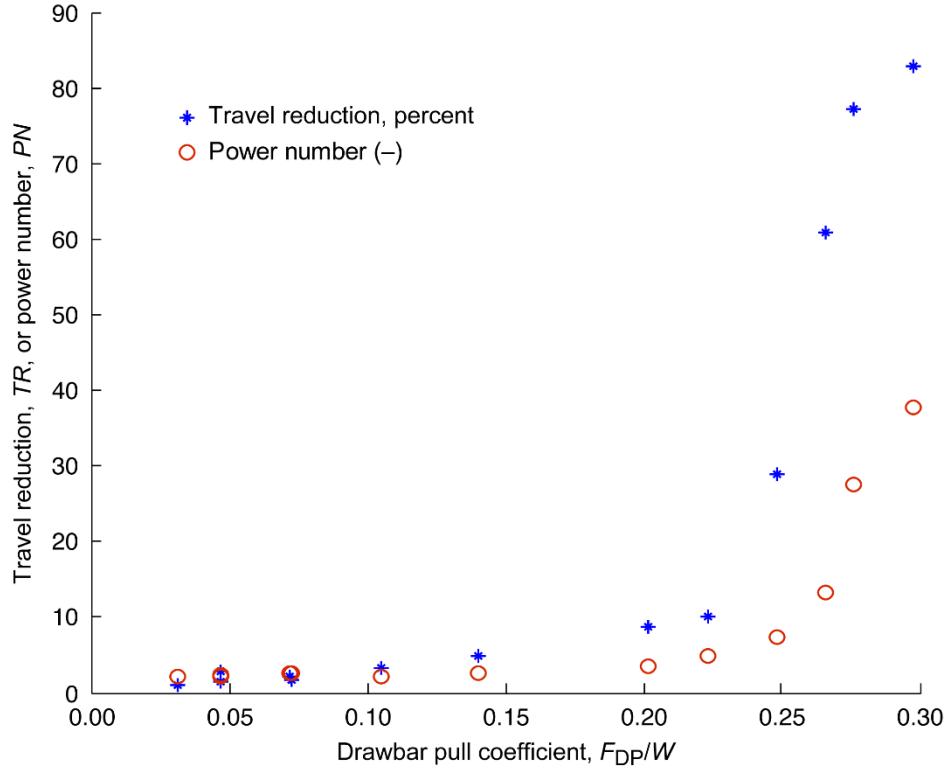

Figure 38.—Complete set of travel reduction and power number results for a single vehicle configuration.

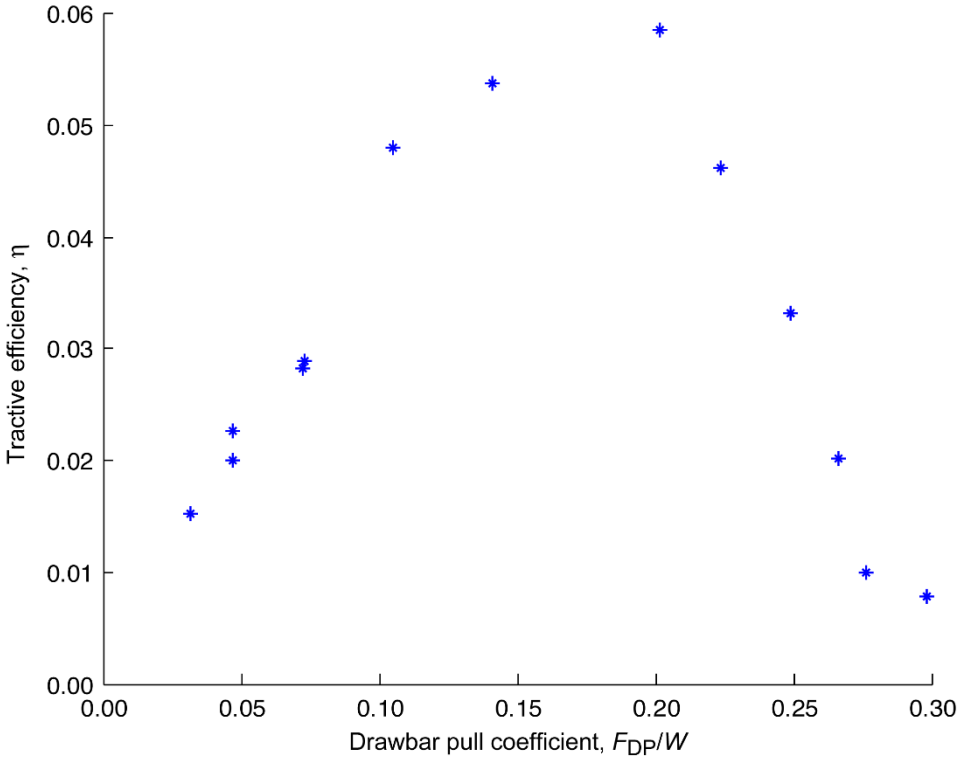

Figure 39.—Tractive efficiency versus drawbar pull (DP) coefficient for a single vehicle configuration.

References

ASAE (2003): General Terminology for Traction of Agricultural Traction and Transport Devices and Vehicles. ASABE S296.5.

Batiste, S.N.; and Sture, S. (2005): Lunar Regolith Simulant MLS–1: Production and Engineering Properties. Lunar Regolith Simulant Materials Workshop Book of Abstracts, Marshall Institute, Madison, AL.

Bekker, Mieczyslaw Gregory (1960): Off-the-Road Locomotion: Research and Development in Terramechanics. University of Michigan Press, Ann Arbor, MI.

Brighton, James, et al. (2006): New Off-Road Dynamics Facility at Cranfield University. Presented at the 10th European Conference of ISTVS, Budapest, Hungary.

Carrier, W.D.; Olhoeft, G.R.; and Mendell, W. (1991): Physical Properties of the Lunar Surface. Lunar Sourcebook, Grant H. Heiken, David T. Vaniman, and Bevan M. French, eds., Cambridge University Press, New York, NY.

Carter, J.L., et al. (2004): Lunar Simulant JSC–1 Is Gone: The Need for New Standardized Root Simulants. Proceedings of the Space Resources Roundtable VI, Lunar and Planetary Institute, Houston, TX, p. 15.

Freitag, D.R.; Green, A.J.; and Melzer, K.J. (1970): Performance Evaluation of Wheels for Lunar Vehicles. U.S. Army Technical Report M–70–2.

Gill, William R.; and Vanden Berg, Glenn E. (1968): Soil Dynamics in Tillage and Traction. U.S. Department of Agriculture, Washington, DC, pp. 368–374.

Gom Optical Measuring Techniques (2013): Pontos Software. http://www.gom.com/3d-software/pontos-software.html Accessed 2013.

Green, A.J. (1967): Performance of Soils Under Tire Loads, Report 5: Development and Evaluation of Mobility Numbers for Coarse-Grained Soils. U.S. Army Technical Report No. 3–666. Available from the U.S. Army Corps of Engineers.

Green, A.J.; and Melzer, K.J. (1970): The Performance of Two Boeing-GM Wheels (GM VII and GM VIII) for the Manned Lunar Rover Vehicle. U.S. Army Waterways Experiment Station, Corps of Engineers, Vicksburg, MS. http://oai.dtic.mil/oai/oai?verb=getRecord&metadataPrefix=html&identifier=ADA032963

Green, A.J.; and Melzer, K. (1971): Performance of Boeing LRV Wheels in a Lunar Soil Simulant. NASA CR–127695, 1971. http://ntrs.nasa.gov

International Organization for Standardization (1983): Earth-Moving Machinery—Method of Test for the Measurement of Drawbar Pull First Edition. ISO 7464.

Janosi, Z.; and Hanamoto, B. (1961): Analytical Determination of Drawbar Pull as a Function of Slip for Tracked Vehicles in Deformable Soils. Proceedings of the First International Conference on Terrain Vehicle Systems, Torino, Italy.

Klosky, J.L., et al. (1996): Mechanical Properties of JSC–1 Lunar Regolith Simulant. Proceedings of the Fifth International Conference on Space, New York, NY, pp. 680–688.

McKay, David S., et al. (1991): The Lunar Regolith. Lunar Sourcebook, Grant H. Heiken, David T. Vaniman, and Bevan M. French, eds., Cambridge University Press, New York, NY, pp. 285–356.

McRae, J.; Powell, C.; and Wismer, R. (1965): Performance of Soils Under Tire Loads, Report 1: Test Facilities and Techniques. U.S. Army, Vicksburg, MS.

Melzer, K. (1971): Measuring Soil Properties in Vehicle Mobility Research: Report 4. Relative Density and Cone Penetration Resistance. Army Engineer Waterways Experiment Station. U.S. Army, Vicksburg, MS.

Meyer, Marvin P.; Ehrlich, I. Robert; and Sloss, David (1977): International Society for Terrain-Vehicle Systems Standards. J. Terramechanics, vol. 14, no. 3, pp. 153–182.

Mitchell, J.K., et al. (1972a): Soil-Mechanics Experiment. Apollo 15 Preliminary Science Report, NASA SP–289, pp. 7–1 to 7–28.

Mitchell, J.K., et al. (1972b): Soil-Mechanics Experiments. Apollo 16 Preliminary Science Report, NASA SP–315, pp. 8–1 to 8–29.

National Aeronautics and Space Administration (2008a): NASA's Newest Concept Vehicles Take Off-Roading Out of This World. http://www.nasa.gov/mission_pages/constellation/main/lunar_truck.html Accessed June 1, 2009.

National Aeronautics and Space Administration (2008b): The ATHLETE Rover. NASA Jet Propulsion Laboratory California Institute of Technology. http://www-robotics.jpl.nasa.gov/systems/system.cfm?System=11 Accessed June 1, 2009.

National Space Science Data Center (2005): Apollo 15 and 16 Soil Mechanics Penetrometer Data. http://nssdc.gsfc.nasa.gov/planetary/lunar/lunar_data/soil_mech_browse.html Accessed June 1, 2009.

Northon, F.E. (1967): Engineer Design Test of Mobility Test Article Model GM–1. NASA CR–103805, 1967. Available from the NASA STI Program.

Oravec, H.A.; Zeng, X.; and Asnani, V.M. (2010): Design and Characterization of GRC–1: A Soil for Lunar Terramechanics Testing in Earth-Ambient Conditions. J. Terramechanics, vol. 47, no. 6, pp. 361–377.

Powell, C.J.; and Green, A.J. (1965): Performance of Soils Under Tire Loads, Report 2; Analysis of Tests in Yuma Sand Through August 1962. U.S. Army Technical Report No. 3–666.

Rimik (2015): CP40II Cone Penetrometers. http://www.rimik.com/cp4011-penetrometer/ Accessed Jan. 24, 2017.

Schreiber, M.; and Kutzbach, H. (2007): Comparison of Different Zero-Slip Definitions and a Proposal To Standardize Tire Traction Performance. J. Terramechanics, vol. 44, no. 1, pp. 75–79.

Sharma, Ajay Kumar; and Pandey, K.P. (1998): Traction Data Analysis in Reference to a Unique Zero Condition. J. Terramechanics, vol. 35, no. 3, pp. 179–188.

Smith, J.L. (1964): Strength-Moisture-Density Relations of Fine-Grained Soils in Vehicle Mobility Research. Issue 3, Part 639 of Technical Report, U.S. Army, Vicksburg, MS.

Turnage, Gerald W.; and Green, J.A. (1966): Performance of Soils Under Tire Loads: Report 4, Analysis of Tests in Sand From September 1962 through November 1963. U.S. Army, Vicksburg, MS.

U.S. Army (1948): Trafficability of Soils: Laboratory Tests to Determine Effects of Moisture Content and Density Variations. U.S. Army Technical Report No. 3–240 suppl.1.

Wettergreen, David, et al. (2010): Design and Field Experimentation of a Prototype Lunar Prospector. Int. J. Robot. Res., vol. 29, no. 12, pp. 1550–1564.

Wong, J.Y. (2010): Terramechanics and Off-Road Vehicle Engineering, Second Edition: Terrain Behaviour, Off-Road Vehicle Performance and Design. Elsevier, Oxford, pp. 134–135.

Wong, J.Y., et al. (1998): Optimization of the Tractive Performance of Four-Wheel-Drive Tractors: Theoretical Analysis and Experimental Substantiation. Proc. Inst. Mech. Eng. D J. Automob. Eng., vol. 212, no. 4, pp. 285–297.

Woodward, Adam Charles (2011): Experimental Analysis of the Effects of the Variation of Drawbar Pull Test Parameters for Exploration Vehicles on GRC–1 Lunar Soil Simulant. Master's Thesis, Virginia Tech.

Zeng, X., et al. (2010): Geotechnical Properties of JSC–1A Lunar Soil Simulant. J. Aerosp. Eng., vol. 23, no. 2.